




Cite this: *J. Mater. Chem. A*, 2017, 5, 15486

Solar-energy-driven conversion of biomass to bioethanol: a sustainable approach

Betina Tabah,^a Indra Neel Pulidindi,^a Venkateswara Rao Chitturi,^b Leela Mohana Reddy Arava,^b Alexander Varvak,^c Elizabeth Foran^c and Aharon Gedanken ^{*a}

Bioethanol is one of the most promising transportation fuels with economic, environmental, and energy benefits. However, currently, the production methodologies and purification technologies of the biofuel industry are not economical. This review demonstrates an economically viable, energy efficient, and sustainable alternative to the state-of-the-art process for bioethanol production from biomass. We have developed a solar-thermal-energy-driven simultaneous saccharification and fermentation (SSF) process for single-step conversion of biomass to bioethanol. In the early stages, aqueous solutions of glucose, starch, or cellulose were fed into a specially designed solar reactor containing instant baker's yeast (*Saccharomyces cerevisiae*) and the necessary enzymes. The yeast (biocatalyst) was not supplemented by any other nutrient, and it was demonstrated that the same yeast and enzymes could be used for at least two months without any decrease in enzymatic activity. After obtaining very high yields (up to 91% of the theoretical yield) and excellent separation of ethanol from the fermentation broth, the methodology was successfully extended to a continuous-flow single-step conversion of marine algae *Ulva rigida* to bioethanol (84% of the theoretical yield). Harnessing solar thermal energy for driving the SSF reaction as well as the special design of the solar reactor that facilitates *in situ* separation of ethanol from the fermentation broth by an evaporation–condensation process make the current method

Received 9th April 2017
Accepted 30th June 2017

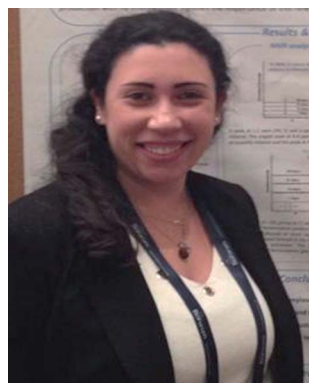
DOI: 10.1039/c7ta03083e

rscl.li/materials-a

^aDepartment of Chemistry, Institute for Nanotechnology and Advanced Materials (BINA), Bar-Ilan University, Ramat-Gan 5290002, Israel. E-mail: gedanken@mail.biu.ac.il

^bDepartment of Mechanical Engineering, Wayne State University, Detroit, MI 48202, USA

^cThe Mina and Everard Goodman Faculty of Life Sciences, Institute for Nanotechnology and Advanced Materials (BINA), Bar-Ilan University, Ramat-Gan 5290002, Israel



Betina Tabah is pursuing her Ph.D. degree under the supervision of Prof. Aharon Gedanken at Bar-Ilan University, Israel. Her thesis work focuses on novel methods for the conversion of biomass to bioethanol. She is passionate about finding green solutions to global problems. Her research interests include potential alternative energy sources, biofuels and renewable energy studies, utilizing

different biomass for energy applications, developing biofuel production systems and up-scaling to industrial applications, and conversion of wastes and plant residues into value-added products. Betina was selected as a 2014 Rieger-JNF Fellow and 2015 Marshall Tulin Fellow in Environmental Studies by the Rieger Foundation, USA.



Indra Neel Pulidindi works as a visiting scientist under the supervision of Prof. Tae Hyun Kim at Hanuyang University, Korea. His research interests include nuclear chemistry, catalysis, materials science, renewable energy, and biofuels. He is passionate about identifying solutions for societal problems such as energy crisis and environmental pollution by means of utilizing natural

resources such as solar energy, CO₂, and biomass. His research focuses on developing alternative renewable energy sources. He is currently working on the conversion of both terrestrial lignocellulosic and algal biomass to biofuels and biochemicals using solar energy for fuel production and lignin valorization.

industrially appealing and adoptable for large-scale production. This review explores new avenues for a decentralized power supply based on solar thermal energy. The bioethanol produced in this study was demonstrated as a potential fuel for direct ethanol fuel cells with high current and power density values, and 65% thermodynamic efficiency. In addition, the secondary metabolite glycerol was fully reduced to the value-added product 1,3-propanediol by *S. cerevisiae*, which is the first example of a fungal strain converting glycerol *in situ* to 1,3-propanediol. In this review, we aim to discuss the current methodologies and recent developments for bioethanol production from biomass and demonstrate the future aspects of bioethanol production in solar reactors, and strategies to improve process yields as well as the prospects of using a solar reactor to produce other valuable chemicals.

1. Introduction

1.1. Bioethanol: one of the best alternatives to petroleum

The indiscriminate extraction and increasing consumption of fossil fuels are considered important triggers in the search for alternative sources of energy that can supplement or replace fossil fuels.¹ Numerous experts predict that the ceiling of oil production will be reached by 2020, while the demand will continue to grow. At the same time, concerns about climate change and the potential economic and political impact of limited oil and gas resources are increasing.² Therefore,

research efforts are being directed towards the use of renewable sources such as solar, wind, and biomass.³

Biofuels are potential substitutes for current transportation fuels. Biofuels from biomass significantly reduce the dependence on imported oil and decrease the environmental impact of energy use.² Major commercial biofuels include bioethanol and biodiesel. Countries such as Brazil and the US have started producing first-generation bioethanol and biodiesel from food products (grains, sugar- or starch-based crops, and edible oil), and these fuels are currently available at petrol stations. Second-generation bioethanol from ligno-cellulosic materials is still under research.⁴ The potential global production of bioethanol from wasted crops and crop residues is estimated at 491 GL per year, which can replace 32% of the total gasoline consumption.⁵

Bioethanol is currently one of the most promising alternatives to conventional transportation fuels because of its high octane value, high combustion efficiency (the anti-knock index for gasoline: 87 and for ethanol: 99), and energy benefits (energy density value of bioethanol: 23 MJ L⁻¹; gasoline: 35 MJ L⁻¹).⁶⁻⁹ In addition, the use of ethanol produced from biomass as a transport fuel can reduce CO₂ buildup.¹⁰ Bioethanol can be blended with petrol (E5, E10 or E85) or used as neat alcohol in dedicated engines.¹¹ Moreover, bioethanol is an excellent fuel for flexible-fuel hybrid vehicles.¹¹ Compared to gasoline, ethanol only contains a trace of sulfur and no nitrogen;

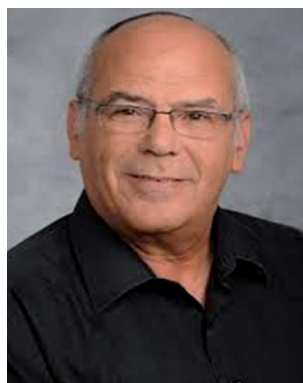


Venkateswara Rao Chitturi is a scientist at Nova-Kem LLC, USA. His research interests include synthesis of nano-materials and organometallic complexes, deposition techniques, fuel cells, rechargeable lithium batteries, and molecular modeling.



Leela Mohana Reddy Arava is an assistant Professor at Wayne State University, USA. His research group is interested in fundamental electrochemical principles underlying energy systems such as batteries, supercapacitors, and fuel cells. His research is focused on designing a variety of nanomaterials and understanding their transport phenomena, electrode kinetics, electrocatalytic activity, and

thermal and electrochemical stabilities under extreme environments. His diverse activities in terms of applications include developing high energy and safe batteries for electric vehicles, micro-batteries to power micro-sensors, and flexible hybrid energy devices for wearable assistive technologies.



Aharon Gedanken is an Emeritus Professor at Bar-Ilan University, Israel. In the EC program FP7, he was the Israeli representative to the Nanotechnology, Materials, and Processes (NMP) committee. He was a partner in 12 EC projects, of which two were coordinated by him. His research interests include sonochemistry, surface coating, synthesis of nanomaterials, microwave superheating, synthesis reactions

under autogenic pressure at elevated temperatures, fuel cells, renewable energy (biomass conversion to biofuels), carbon materials, sensors, medicinal chemistry, and polymers. Gedanken has published 770 papers in peer-reviewed journals. Prof. Gedanken is the recipient of 2009 Israel Vacuum Society and 2012 Israel Chemical Society awards of excellence in research.

therefore, ethanol blended with gasoline helps to decrease the overall emission of sulfur oxides (SO_x) and nitrogen oxides (NO_x).¹²

Currently, bioethanol is the most dominant biofuel, and its global production has shown an upward trend over the last 25 years, with a sharp increase from the year 2000 onwards. Global annual bioethanol production has reached nearly 115 billion liters in 2015.¹³ Bioethanol production is important not only for transportation applications, but also for its use as a feedstock for the production of C₂ hydrocarbons. In the near future, biofuels – especially bioethanol – may be a vital feedstock for long-chain hydrocarbons and biochemicals that are currently derived from petroleum.^{14,15} Therefore, any breakthrough in bioethanol-production technology is beneficial to the socio-economic well-being of humankind. It is important to note that the use of bioethanol as an alternative fuel is not yet economically competitive with petroleum-based fuels. Major drawbacks of commercial bioethanol production include broad variation in the chemical composition of the feedstock, inherent slowness of the fermentation reaction, the separation of microorganisms (yeast) from the fermentation broth, and the separation and purification (distillation) of ethanol in an energy-efficient way. The main strategies for increasing the competitiveness of bioethanol as an alternative fuel include finding a cheap and abundant feedstock and developing a technology that is more atom- and energy-efficient than the currently available processes.¹⁶

1.2. Potential feedstocks for bioethanol production

Two processes are involved in the conversion of biomass to ethanol: the degradation of the starting plant material into fermentable sugars (hydrolysis) and the conversion of sugar into alcohol (fermentation).^{17–19} The selection of the suitable feedstock for fermentable sugars is a challenge. The varied raw materials used in the manufacture of ethanol *via* fermentation are classified into three main types: sugars, starches, and cellulosic materials.²⁰ Currently, the global ethanol supply is produced mainly from sugar and starch.²¹ Glucose is the basic sugar unit in biomass that can be obtained from the hydrolysis of cellulose and starch. Glucose is highly water-soluble, which not only makes its transportation very convenient for chemical engineering operation, but also enables the products to be highly concentrated. Furthermore, glucose does not need to undergo the rate-determining step of hydrolysis during catalytic conversion.^{22,23} Sucrose is the main sugar extracted from sugar cane and sugar beets, and is highly soluble in water. Ethanol production from sucrose predominates in tropical regions with sugar cane production such as Brazil.²⁴ Industrial strains of yeast such as *Saccharomyces* can be used to hydrolyze sucrose into fructose and glucose and ferment the sugars into ethanol. *Saccharomyces cerevisiae* is the most effective ethanol-producing microorganism for hexose sugars, including glucose, mannose, and galactose.^{25,26}

Starch is an excellent carbon source and a major energy-storage molecule (60–75 wt%) for many economically important crops such as corn, wheat, oats, rice, potatoes, and

cassava.^{27–29} The fermentation of starch is more complex than the fermentation of sugars, because starch must be hydrolyzed to glucose before it can be fermented to ethanol.^{27,28} This two-step process can be made more economical by coupling the enzymatic hydrolysis of starchy substrates and the fungal fermentation of the derived glucose into a single step by a simultaneous saccharification and fermentation (SSF) process. In the SSF process, the stages are the same as those in separate hydrolysis and fermentation systems, but both are performed in the same reactor.^{30–34} This causes less accumulation of sugars within the reactor, a greater yield of ethanol, and a higher saccharification rate.³⁵ Another advantage of this approach is that only a single container (fermentor) is needed for the entire process, which decreases the investment costs.³⁶ In addition, the presence of ethanol in the culture medium causes the mixture to be less vulnerable to undesired microorganism invasion.³⁷

Among the three main types of raw materials, cellulose materials are the most abundant global source of biomass and have been largely unutilized. Over 90% of the global production of plant biomass is lignocellulose, which is a more complex substrate than starch.¹¹ Lignocellulose is composed of a mixture of carbohydrate polymers (cellulose and hemicellulose) and lignin.¹⁹ The biological process for converting the lignocellulose to fuel ethanol requires delignification to liberate cellulose and hemicellulose from their complex with the lignin, depolymerization of the carbohydrate polymers to produce free sugars, and the fermentation of mixed hexose and pentose sugars to produce ethanol. Although cellulose can be effectively utilized for bioethanol production, hemicellulose conversion to bioethanol still remains a challenge.^{11,19,38} Extensive research has been carried out in this field for the selective isolation of cellulose in a cost-effective and environmentally friendly manner.³⁹ It is expected that the cost of lignocellulosic ethanol can undercut that of starch-based ethanol, as the low-value agricultural residues can be used as a feedstock.^{20,40} It is noteworthy that *S. cerevisiae* has high ethanol productivity and high tolerance to the inhibitory compounds and ethanol present in the hydrolysate of lignocellulosic biomass.³⁶ Developing technologies that can convert cellulosic materials into motor fuels has been a worldwide goal of governments and private industries for the last three decades; however, cellulosic ethanol production is still in the exploratory stage.^{33,41,42}

Considered to be the third-generation biomass, algae have proven to be superior to other biomass due to their environmental and economic sustainability. Marine algae hold promise as an alternative, renewable feedstock for the production of biofuels, especially bioethanol.⁴³ Marine macroalgae (seaweeds) can serve as a promising sustainable source for biofuels due to their high growth rates and productivity, low energy demand, low lignin content, and high carbohydrate content. Algae-based biofuels, as opposed to terrestrial biomass sources, do not compete with the cultivation of food crops or freshwater supply, nor adversely affect vulnerable ecosystems.^{43–45} The potential of seaweeds, such as *Gelidium amansii*, *Laminaria japonica*, *Codium fragile*, *Nizimuddiniana zanardini*, and *Ulva rigida*, has been exploited for bioethanol production.³³ Although seaweeds are

promising feedstocks for biofuel production, their relatively low readily available fermentable carbohydrate content compared to their terrestrial counterparts, and the inefficient methods used for their farming and conversion, hinder their utilization in the biofuel industry.³⁴ Thus, developing novel approaches to produce biofuels from macroalgal biomass may have a tremendous impact on the possibility of using this feedstock as a future renewable energy source.⁴⁵ The green macroalga *Ulva* (Chlorophyceae) is a common marine alga found abundantly in eutrophicated coastal waters. This marine alga is an important source of dissolved organic carbon (carbohydrates, polysaccharides, and nitrogenous and polyphenolic materials) and can be considered as a potential energy crop due to its high growth rates and relatively high carbohydrate content (~40%).^{34,46}

1.3. Current methodologies for bioethanol production

Currently, the only available pathway for the conversion of carbohydrates into ethanol is the biological pathway, *i.e.* fermentation, which is the most time-consuming part of the bioethanol production process. There are many reports in the literature that focus on the evaluation of different carbohydrates and fermentation conditions for accelerated bioethanol production.^{31,33,34,42,44,47–49} Ultrasonication has been widely applied for accelerating biological and chemical processes.³ Ultrasound-assisted hydrolysis has been shown to intensify and improve the efficiency of the process and to considerably reduce the extraction time.³³ Microwave irradiation has also been demonstrated to accelerate the release of fermentable sugar from biomass.⁴³ Localized heating during microwave irradiation causes biomass degradation and, as a result, the catalytic species to access the reaction site, which leads to the release of monosaccharides. Use of microwave irradiation saves time and energy because the target compounds are heated directly, without the need to heat a furnace or oil bath as required in conventional heating methods.⁴³ To summarize, the current bioethanol production methods are mostly based on highly controlled reactions and state-of-the-art instruments such as a sonicator, incubator, high-speed stirrer or microwave.⁵⁰ This review demonstrates an environmentally benign process for bioethanol production. In our current study, solar energy was used as a heating element for the catalyst and reaction volume, replacing an oven or a heating plate. In the same way, the separation step was aided by solar energy, as the ethanol produced in the reactor was separated from the broth soon after its formation by an evaporation–condensation process.

1.4. Solar-energy-driven bioethanol production

An ideal heating source for the fermentation process should complete the reaction in a short time and be energy efficient. Moreover, to reach industrial quantities of the product, the heating source must be suitable for industrial applications.^{51,52} In most biofuel-production processes, reaction temperatures are attained by the use of electricity, which results in a considerable increase in the production cost.⁵³ Renewable energy sources, such as solar, wind, geothermal, and biomass, can be used to

supplement power to biorefineries, lower production cost, and improve the net energy ratio. Among these sources, solar energy, with the advantages of abundance and availability, is an excellent candidate for supplementing biofuel production.⁵⁴

The conversion of solar energy into chemical energy, photosynthesis, is the basis for life. Photosynthesis fills all of the food requirements and many of the needs for fiber and building materials. The energy stored within fossil fuels is also based on chemical energy that comes from the sun *via* photosynthesis. In order to provide new and efficient ways to collect and utilize solar energy, the energy-harvesting systems of plants can be adapted to man-made systems.^{18,55} In the 21st century, it is crucial to have a successful transition to clean well-regulated independent energy. Solar energy may be an important alternative energy source and may provide a solution to the growing energy demand, even if only a small portion of this source is harnessed for heating applications.^{31,47} This study uses renewable solar thermal energy as a heating source to power the production of bioethanol. Using solar thermal energy for bioethanol production has economic and environmental advantages, as it reduces much of the electricity costs associated with the process, resulting in cost-effective sustainable green production. Therefore, the utilization of solar thermal energy for biofuel production has a significant impact on the overall energetics (energy return on energy invested, EROEI) of the process. To the best of our knowledge, we are the first to utilize solar energy for bioethanol production.^{31,47,50} This review demonstrates a solar reactor that converts carbohydrates into bioethanol in batch and continuous-flow processes. Bioethanol is produced from glucose through continuous-flow solid-state fermentation, as well as from starch, cellulose, and marine algae (*Ulva rigida*), through single-step SSF processes performed in a solar-energy-driven reactor. Moreover, the bioethanol produced is demonstrated as a potential fuel for operating direct ethanol fuel cells (DEFCs).^{31,47}

2. Solar reactor

2.1. Design and fabrication

A solar reactor was designed and fabricated to perform either continuous-flow or batch fermentation of biomass and to continuously separate the product (aqueous ethanol) from the yeast bed by an *in situ* evaporation–condensation mechanism (see Fig. 1 for a detailed design and depiction of the components of the solar reactor).^{31,47} The selected geometry and the dimensions are the most important aspects of the reactor for the effective production and separation of ethanol. The reactor was fabricated in the mechanical workshop of Bar-Ilan University using aluminum blocks and a glass lid. The height of the reactor (127 mm) was kept much lower than the base (275 mm) to facilitate the condensation of the ethanol vapor (from the first chamber) onto the top glass surface (Fig. 1a). Such a geometry facilitates the free flow of the condensate from the top glass surface of the reactor to the second chamber, where ethanol is collected. The ethanol collection chamber (second chamber) is fully separated from the fermentation chamber (first chamber) by an aluminum wall (Fig. 1b). The inlet of the

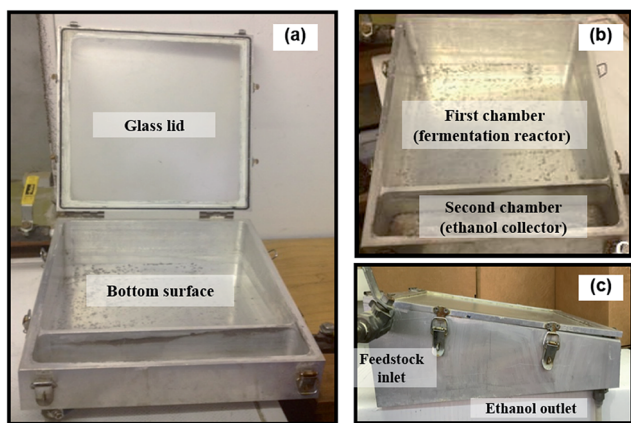


Fig. 1 Open reactor (a), the bottom surface with two chambers (b), side view of the reactor (c).⁵⁸ Adapted with permission.³¹ Copyright 2015 John Wiley and Sons, Inc.

reactor is connected to the feed reservoir and the ethanol outlet valve is opened to collect the product ethanol at regular time intervals (Fig. 1c). The secondary metabolites remaining in the fermentation broth can be collected from an additional outlet, connected to the fermentation chamber, without opening the reactor lid.

2.2. Principle of operation

The normal boiling-point temperature (T , °C) is related to the vapor pressure (P , mmHg) of ethanol according to the Antoine equation, $\log_{10} P = A - (B/(C + T))$, where A , B , and C are substance-specific coefficients. The equation can be rearranged as $P = 10^{A - (B/(C + T))}$. The constants for ethanol for the temperature range of 0–100 °C are $A = 8.04494$, $B = 1554.3$, and $C = 222.65$.⁵⁶ The temperature–pressure plot for ethanol is depicted in Fig. 2 according to the following formula: $P = 10^{8.04494 - (1554.3/222.65 + T)}$.⁵⁶ In the current study, the evaporation–condensation process occurs at a reaction temperature (20–35 °C) much lower than the boiling point of ethanol (78 °C). Although the pressure during fermentation was not monitored using a pressure gauge, it can be concluded that the pressure in the reactor is much lower than the atmospheric pressure.^{31,47,50}

3. Solar-energy-driven fermentation of carbohydrates

3.1. Solar-energy-driven SSF in a batch process

For the efficient utilization of solar energy, and for the SSF process to be cost-effective, our work focuses on using solar thermal energy for the conversion of biomass into ethanol in a single-step process in the solar reactor. From the green chemistry point of view, the solar-energy-driven SSF process has numerous advantages. The reaction time is short, due to the coupling of the hydrolysis and fermentation stages into one stage. The SSF process is more economical because both the hydrolysis and fermentation stages are performed in the same reactor. The process does not require either an external source

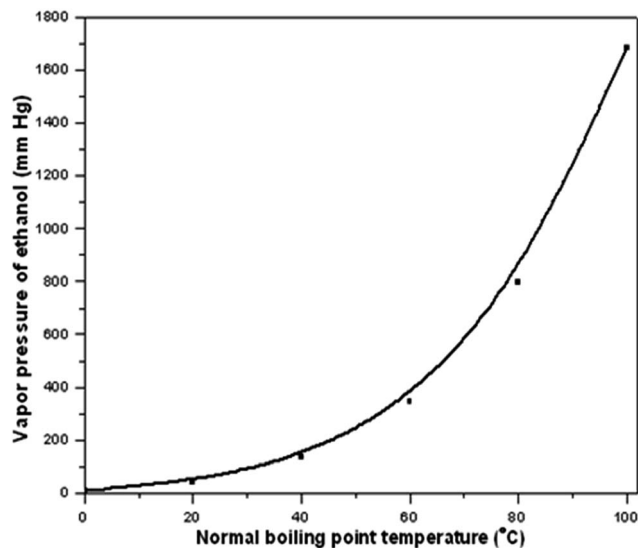


Fig. 2 The vapor pressure of ethanol vs. the normal boiling-point temperature. Reprinted with permission.³¹ Copyright 2015 John Wiley and Sons, Inc.

of heating or additional energy and does not produce any polluting effluent. Successful results and high bioethanol yields were obtained from solar-energy-driven SSF of starch, cellulose, and the marine algae *Ulva rigida* in batch processes.

3.1.1. SSF of starch to bioethanol in a batch process. A homogeneous aqueous suspension of starch (5 wt%, 1.6 L) was prepared under stirring and heating using a high-speed ultraturrax device. The starch solution obtained was fed into the reactor charged with *S. cerevisiae* (instant baker's yeast purchased from a local supermarket) covered with an activated carbon cloth and a mixture of amyloglucosidase and α -amylase enzymes.³¹ The conversion of potato starch to ethanol through an SSF process involves the simultaneous hydrolysis of starch to glucose by the action of enzymes and fermentation of glucose by yeast. The first biomass conversion step usually involves a hydrothermal pretreatment before enzymatic hydrolysis; however, in the current study, no hydrothermal pretreatment was applied before the SSF process and the yeast was not supplemented with any additional nutrients.^{31,57} The ethanol produced was evaporated to the top flat glass surface of the reactor, allowing the solar radiation into the fermentation chamber. The ethanol droplets condensed on the glass plate were collected in the second chamber of the reactor which has an outlet for ethanol collection (Fig. 1). The process was monitored for over two months (63 days) in the solar reactor at 30–35 °C. The analytes were collected at regular time intervals and analyzed for quantification of the ethanol using proton (^1H) NMR spectroscopy and gas chromatography (GC). The change in ethanol yield with time (deduced from ^1H NMR analysis) is depicted in Fig. 3. The concentration of ethanol varies over the range of 1.8–2.6 wt% over the course of the study. By the 63rd day, 38 g of ethanol were collected in total (0.6 g ethanol per day, 8 g ethanol per m² per day), which corresponds to ~85% of the theoretical yield of ethanol from starch with green chemistry

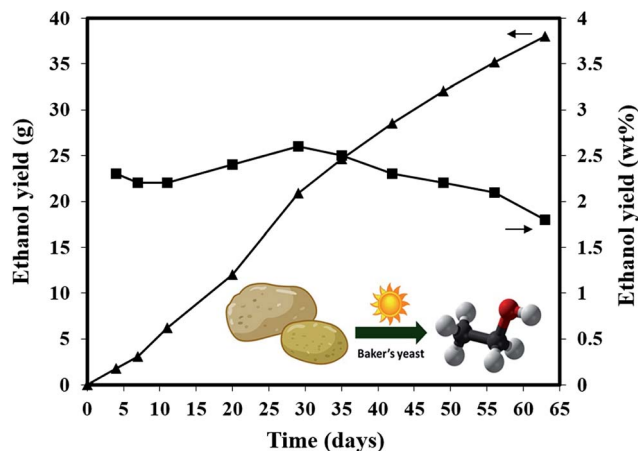


Fig. 3 Solar-energy-driven bioethanol production from 5 wt% starch solution as a function of time. Adapted with permission.³¹ Copyright 2015 John Wiley and Sons, Inc.

metrics RME = 47.4% and MI = 0.85 (Table 1). The mass-balance calculations and detailed gas chromatograms of SSF products collected at regular time intervals were reported by Tabah *et al.*³¹ The weekly ethanol concentration in the products, determined from the ¹H NMR (0.42–0.60 M) and GC (0.39–0.56 M) analyses, confirms the authenticity of the methodology used for ethanol estimation.^{31,50}

Representative ¹H NMR spectra of the analytes collected on the 7th, 14th, 21st, and 28th days of the SSF process are shown in Fig. 4. Signature peaks of ethanol centered at 1.19 ppm (3H, t) and 3.66 ppm (2H, q) were observed in all the analytes (Fig. 4a–d). The singlet peak at 8.40 ppm originates from the internal standard HCOONa, and the peak at 4.80 ppm corresponds to water. No reaction by-products (glycerol or acetic acid) were observed in the analytes, indicating the purity of the process (only aqueous ethanol). In addition to the quantitative methods, the SSF product was analyzed qualitatively by carbon (¹³C) NMR spectroscopy. The ¹³C NMR spectra of the SSF products collected weekly were compared to those of commercial ethanol.^{31,50} No peaks other than the characteristic peaks of ethanol (at 17 and 58 ppm) were observed in the reaction products. This indicates that the reaction product is pure

aqueous ethanol and is devoid of the reactant (starch), reaction intermediate (glucose), and usual secondary metabolites of fermentation (glycerol and acetic acid). The SSF process was then scaled up to 15 wt% starch to produce a more concentrated bioethanol (1.3 M, 6 wt%) that can be evaluated as a fuel in DEFCs. The total amount of ethanol at the end of the process was 71.2% of the theoretical yield with green chemistry metrics RME = 39.8% and MI = 0.71 (Table 1). The fuel cell tests successfully demonstrated that as-produced bioethanol from the solar-energy-driven SSF process of 15 wt% starch (2.9 g ethanol per day, 37.7 g ethanol per m² per day) is a potential fuel for DEFCs.³¹

3.1.2. SSF of cellulose to bioethanol in a batch process. A homogeneous aqueous suspension of cellulose (5 wt% Avicel® PH-101, 1 L) was prepared under sonication (1 h, high-intensity ultrasonic Ti-horn). After the sonication process, a well-dispersed stable suspension of cellulose was used as a feedstock for the SSF process in the solar reactor. The cellulose solution was fed into the reactor charged with *S. cerevisiae* (instant baker's yeast) covered with an activated carbon cloth and a mixture of endo-cellulase, exo-cellulase, and β-glucosidase enzymes. The conversion of cellulose to ethanol through an SSF process involves the simultaneous hydrolysis of cellulose to glucose by the action of enzymes and the fermentation of glucose by yeast. In the current study, no hydrothermal pretreatment was applied before the SSF process of cellulose and the yeast was not supplemented with any additional nutrients. The process was monitored for 10 days in the solar reactor at an average day/night temperature of 27/15 °C. The analytes were collected at regular time intervals and analyzed for the quantification of ethanol using ¹H NMR spectroscopy and high performance liquid chromatography (HPLC). The change in ethanol yield with time (deduced from ¹H NMR analysis) is depicted in Fig. 5 (unpublished data).

The concentration of ethanol varied over the range of 2.0–2.40 wt% over the course of the study. By the 10th day, 22 g of ethanol was collected in total (2.2 g ethanol per day, 28.9 g ethanol per m² per day), which corresponds to 78% of the theoretical yield of ethanol from cellulose with green chemistry metrics RME = 43.7% and MI = 0.78 (Table 1). The ethanol concentration of the products, determined from ¹H NMR

Table 1 Bioethanol yields and green chemistry metrics for various feedstock and fermentation types

Feedstock	Type of fermentation	Feedstock concentration (wt%)	Ethanol yield (g per day)	Ethanol yield (theoretical%)	RME ^a (%)	MI ^b	Ref.
Glucose (D-glucose)	Continuous flow	10	3.71	91.2	46.5	0.91	47 and 50
		20	7.01	85.5	43.6	0.86	
		30	10.9	89.0	45.4	0.89	
		40	14.4	88.0	44.9	0.88	
Starch (potato)	Batch	5	0.60	84.7	47.4	0.85	31 and 50
		15	2.85	71.2	39.8	0.71	
Cellulose (Avicel®)	Batch	5	2.19	78.0	43.7	0.78	Unpublished data
Marine macroalgae (<i>Ulva rigida</i>)	Batch	10	0.41	65.0	11.4	0.65	Unpublished data
	Continuous flow	5	0.20	84.1	15.0	0.84	58

^a Reaction Mass Efficiency (RME)% = (mass of ethanol × 100)/(mass of feedstock). ^b Mass Intensity (MI) = total mass in process/mass of ethanol.

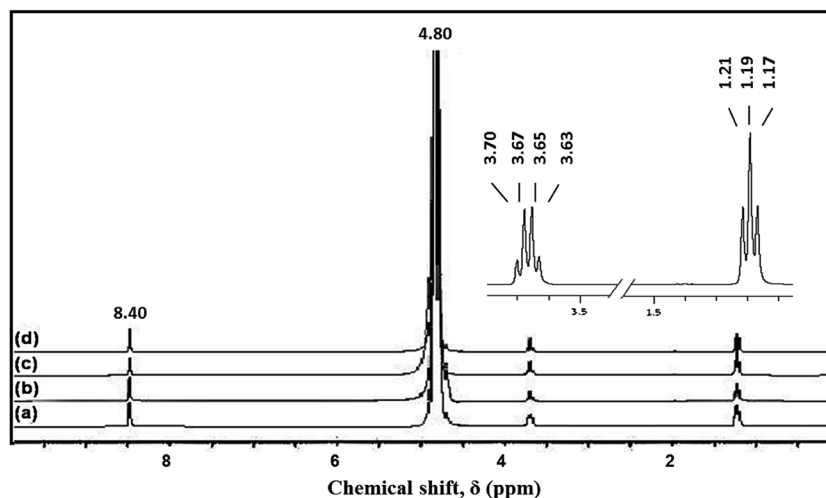


Fig. 4 ^1H NMR spectra of the SSF product on the 7th (a), 14th (b), 21st (c), and 28th (d) days (inset shows the ethanol peaks, a 3H (t) centered at 1.19 ppm and a 2H (q) centered at 3.66 ppm). Reprinted with permission.³¹ Copyright 2015 John Wiley and Sons, Inc.

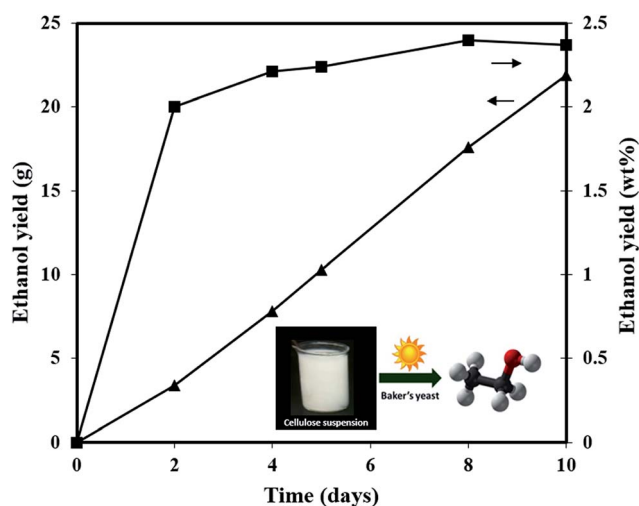


Fig. 5 Solar-energy-driven bioethanol production from 5 wt% cellulose solution (unpublished data).

(0.40–0.60 M) and HPLC (0.43–0.52 M) analysis matched well. The SSF product was also analyzed by ^{13}C NMR spectroscopy and the NMR spectra of the SSF products, collected every other day, were compared with those of commercial ethanol. As in the case of the SSF process of starch, no peaks other than the characteristic peaks of ethanol (at 17 and 58 ppm) were observed in the reaction products. This indicates that the reaction product is pure aqueous ethanol and is devoid of the reactant (cellulose), reaction intermediate (glucose), and usual secondary metabolites of fermentation (glycerol and acetic acid).

3.1.3. SSF of marine macroalgae *Ulva rigida* to bioethanol in a batch process. Fresh wet biomass of marine macroalgae *Ulva rigida* was dried in a hot air oven. The dried biomass was ground in a blender to obtain a fine powder. The *Ulva rigida* powder was then passed through a sieve to obtain biomass particles of uniform size prior to the SSF process (Fig. 6). Initially, an aqueous suspension of *Ulva rigida* (10 wt%) was fed

into the solar reactor to test the solar-aided batch fermentation of marine macroalgae. In this solar-aided SSF process, a mixture of α -amylase, amyloglucosidase, endo-cellulase, exo-cellulase, and β -glucosidase enzymes was added to the feedstock solution, which was fed into the reactor's first chamber over *S. cerevisiae* (instant baker's yeast) covered with an activated carbon cloth.⁵⁸

The chemical composition of the marine macroalgae *Ulva rigida* was analyzed on a dry weight basis. The total carbohydrate content was $37 \pm 3.9\%$, with $7.6 \pm 1.1\%$ starch and $23.8 \pm 1.2\%$ cellulose.³³ Theoretically, based on the cellulose and starch content of *Ulva rigida*, $\sim 32\%$ of the dry biomass should be hydrolyzed to fermentable sugars. The remaining fraction of the carbohydrates should correspond to the structural carbohydrate component ulvan, which is known to yield monosaccharides such as rhamnose.³³ The SSF process of 10 wt% *Ulva rigida* was monitored for 55 days in the solar reactor (with the same enzymes and yeast) at an average day/night temperature of 28/20 °C. The aliquots of the products were collected at regular time intervals and quantified for ethanol using ^1H NMR spectroscopy and HPLC. The ethanol yield (deduced from ^1H NMR analysis) as a function of time is depicted in Fig. 7 (unpublished data). Based on the fermentable sugar content of the biomass, 65% of the theoretical ethanol yield was collected at the end of the SSF process of 10 wt% *Ulva rigida* (0.41 g ethanol per day, 5.4 g ethanol per day per m^2) with green

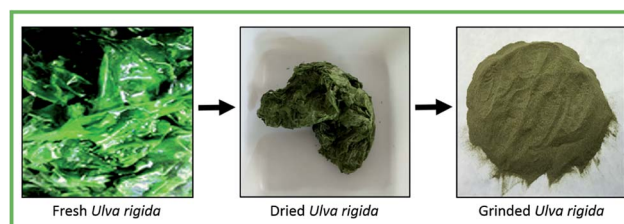


Fig. 6 Fresh (wet), dried, and ground *Ulva rigida* samples.⁵⁸

chemistry metrics RME = 11.4% and MI = 0.65 (Table 1). As previously seen in the SSF of starch and cellulose, no peaks other than the characteristic peaks of ethanol were observed in the ^1H and ^{13}C NMR spectra of the reaction products of the SSF of *Ulva rigida*. This indicates that the reaction product is again pure aqueous ethanol and is devoid of the reactants (starch and cellulose), reaction intermediate (glucose), and usual secondary metabolites of fermentation (glycerol and acetic acid). Following the preliminary results of the batch fermentation, the system was further developed into a solar-energy-driven continuous-flow fermentation process in order to increase the ethanol yield and make the process industrially adoptable.⁵⁸

3.2. Solar-energy-driven SSF in a continuous-flow process

Following the successful results and high ethanol yields with solar-energy-driven SSF of starch, cellulose, and the marine algae *Ulva rigida*, the batch process of bioethanol production was further developed into a continuous-flow process. The process was tested with glucose (10–40 wt%) and *Ulva rigida* (5 wt%) as feedstocks.^{47,50,58}

3.2.1. Fermentation of glucose to bioethanol in a continuous-flow process. Continuous-flow glucose fermentation was performed by feeding the reactor with 2 L of either 10, 20, 30 or 40 wt% aqueous glucose solutions.^{47,50} The reactor was charged with *S. cerevisiae* (instant baker's yeast) into which the glucose solution was continuously fed (2.8 mL h^{-1} flow rate). It is important to note that the yeast was not supplemented with any additional nutrients and the pH of the glucose solutions was 7. As in the case of the previous solar-energy-driven SSF processes, the fermentation took place in the first chamber and the ethanol produced evaporated to the top flat glass surface of the reactor, which allowed the solar radiation to enter the bed. The ethanol droplets that condensed on the glass plate were collected in the second chamber of the reactor, which has an outlet for ethanol collection. For each glucose solution, the process was monitored for a month in the solar reactor at $\sim 20\text{ }^\circ\text{C}$.^{47,50}

The analytes were collected at regular time intervals and analyzed for the quantification of ethanol using ^1H NMR

spectroscopy, GC, and, HPLC. The concentrations of analytes determined by each analysis matched well, validating the methodology used for ethanol estimation.^{47,50} The concentration of aqueous ethanol (ethanol yield, wt%), collected at regular time intervals using 10–40 wt% glucose feed, is depicted in Fig. 8. High ethanol yields (average of 91, 86, 89, and 88% of the theoretical yield, respectively) indicate the atom efficiency of the process. The daily ethanol yield and the green chemistry metrics (RME and MI values) are also calculated and reported in Table 1. It is noteworthy that the yeast bed was always in a solid-state condition (almost complete absence of free water), in which the system had enough moisture to support the growth and metabolism of the microorganisms, and glucose was the only nutrient supplied for the yeast.^{47,50} Solid-state fermentation, with its low-energy requirements, produces less wastewater and is environment-friendly. In addition, the microbial cultures (biocatalysts) are closer to their natural habitats and it is easy to separate them from the broth.⁵⁹ A common problem in bioethanol production is the separation of microorganisms from the broth. Since the recovery of the biocatalysts is simple in solid-state fermentation, the same biocatalyst can be reused for many fermentation cycles.⁶⁰ There was no effluent in the reactor, which made it very convenient to change the feed solutions between the experiments. Moreover, there was no loss in the activity of the yeast even after two months of continuous operation of the process. Fig. 9 shows the HPLC chromatograms of the fermentation product (collected on the 21st day), using 10–40 wt% glucose solutions (Fig. 9b–e) in comparison to commercial ethanol (0.5 M, retention time of ~ 25 min, Fig. 9a). The concentrations of the produced bioethanol are 1, 2, 3, and 4 M from 10, 20, 30, and 40 wt% glucose fermentation, respectively. These high ethanol concentrations indicate the atom efficiency of the process.^{47,50}

In addition to these quantitative methods, the fermentation product was also analyzed by ^{13}C NMR spectroscopy. Fig. 10 shows the ^{13}C NMR spectra of the fermentation products obtained from 10–40 wt% aqueous glucose feed solutions (collected on the 10th day) compared to commercial ethanol.

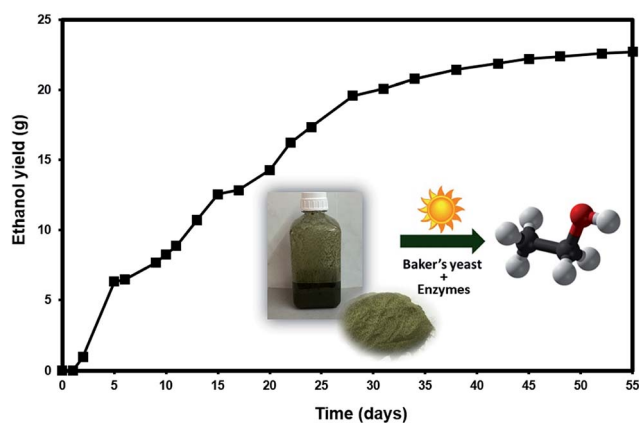


Fig. 7 Solar-energy-driven bioethanol production from batch fermentation of *Ulva rigida* (10 wt%) as a function of SSF process time (T_{ave} day/night: 28/20 $^\circ\text{C}$) (unpublished data).

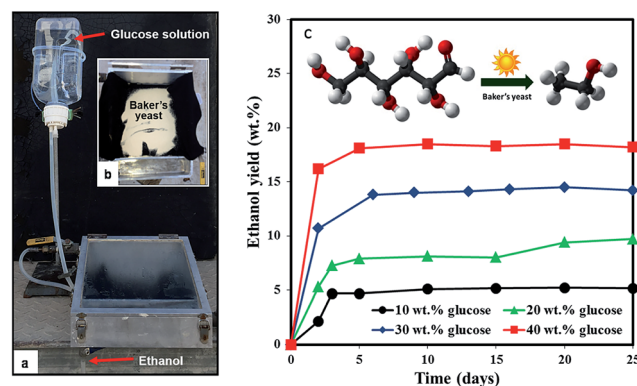


Fig. 8 Continuous-flow solar reactor with a D-glucose reservoir (a), open reactor with instant baker's yeast on activated carbon cloth (b), time on stream studies of ethanol yield (wt%) with 10–40 wt% glucose feed solutions (c). Adapted with permission.⁴⁷ Copyright 2016 Royal Society of Chemistry.

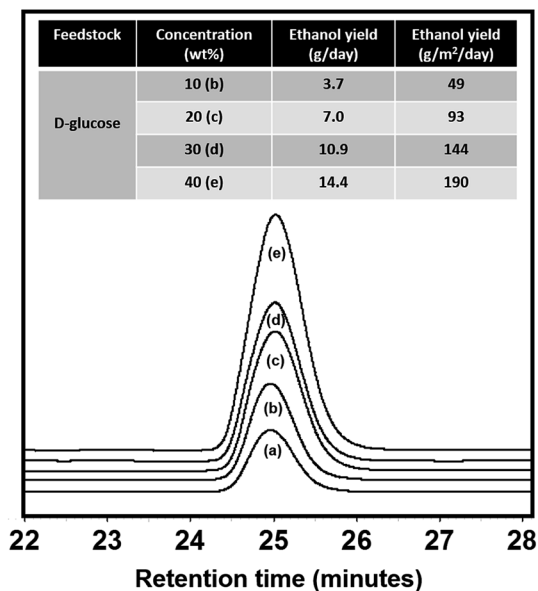


Fig. 9 HPLC chromatograms of commercial ethanol (a) and fermentation products (collected on the 21st day) using 10 (b), 20 (c), 30 (d), and 40 (e) wt% glucose solutions.⁵⁰

Intense signals, typical of the target product ethanol, can be seen in all samples at 17 and 58 ppm (Fig. 10b–e). No peaks other than ethanol appear in the reaction products. The absence of the reactant (glucose) or yeast in the product signifies the role of solar radiation in separating the aqueous ethanol formed in the fermentation chamber by means of evaporation and condensation. The absence of typical peaks of the usual secondary metabolites, glycerol and acetic acid, again indicates the product purity and its possible direct use for energy-related applications such as fuel cells.^{47,50}

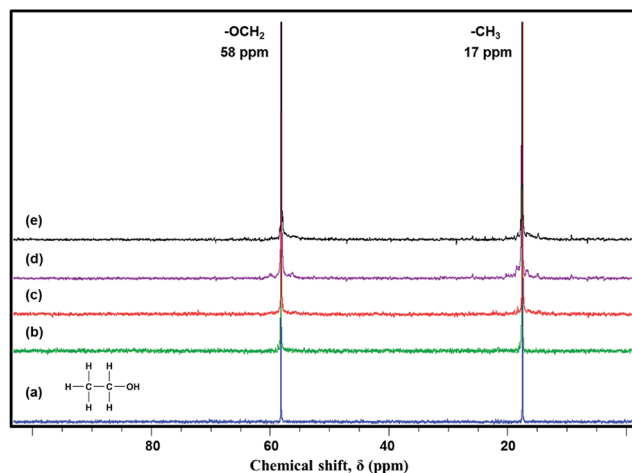


Fig. 10 ¹³C NMR spectra of commercial ethanol (a) and bioethanol collected on the 10th day of the fermentation of 10 wt% glucose solution (1.1 M) (b), 20 wt% glucose solution (1.8 M) (c), 30 wt% glucose solution (3.0 M) (d), and 40 wt% glucose solution (4.0 M) (e). Adapted with permission.⁴⁷ Copyright 2016 Royal Society of Chemistry.

One of the main issues associated with bioethanol production is its purification from the fermentation broth.⁶¹ Ethanol concentration greater than 4% has been a limitation in the conventional fermentation processes, poisoning yeasts and inducing stress by retarding their productivity of further ethanol production.^{48,49} Various approaches are being studied for the extraction and distillation of ethanol (such as liquid–liquid extraction using ionic liquids, the use of microfiltration, and the substitution of membrane technology for current ethanol-dewatering processes).^{61,62} Although further distillation is needed to attain anhydrous ethanol, the unique advantage of the use of solar energy in the current methodology is that no additional extraction process is required to separate the aqueous ethanol from the fermentation broth. The formed ethanol in the yeast bed is simultaneously evaporated and condensed onto the glass panel of the reactor, from which it flows down into a separate chamber with an outlet for ethanol collection (Fig. 1). The pressure in the reactor, which is lower than atmospheric pressure, facilitates the evaporation of ethanol at a temperature much lower than its boiling point (78 °C). The relation between the lowering of the boiling point of ethanol and the pressure of its vapor, as well as the operation principle of the reactor, were discussed in Section 2.2 (Fig. 2). The solar-energy-based fermentation demonstrated in this review offers a solution to the ethanol tolerance limitation by the *in situ* evaporation–condensation process of the target product ethanol, resulting in its separation from the broth. Moreover, the issue of substrate (sugar) inhibition was also solved with the help of this methodology. Aqueous suspensions of glucose with a wide range of concentrations (up to 40 wt%) were fed to the reactor and the highest ethanol concentration obtained was 18 wt%, which was much greater than the 4 wt% limit.^{47,50}

3.2.2. SSF of *Ulva rigida* to bioethanol in a continuous-flow process. A 500 mL slurry of 5 wt% *Ulva rigida* in doubly distilled water (DDW) was sonicated for 90 min using a high-intensity ultrasonic Ti-horn. After the sonication process, a well-dispersed stable suspension of marine algae was obtained and subsequently used as a feedstock for the continuous-flow SSF process in the solar reactor (Fig. 11).⁵⁸ The aqueous suspension of *Ulva rigida*, prepared by ultrasonication, was mixed with α -amylase, amyloglucosidase, endo-cellulase, exo-cellulase, and β -glucosidase enzymes and fed to the fermentation chamber of the solar reactor (at a flow rate of 3.9 mL h⁻¹), loaded with instant baker's yeast (*S. cerevisiae*) that was covered with activated carbon cloth. In this solar-energy-driven continuous-flow SSF process, the enzymes induced the hydrolysis of the starch and cellulose components of the algae to glucose, which was further fermented by the yeast and converted to ethanol. When 500 mL *Ulva rigida* feedstock was completely fed to the reactor, DDW was streamed through the reactor (with the same flow rate, 3.9 mL h⁻¹) in order to convert the residual carbohydrates of the algae to bioethanol. When the DDW was completely used up, an additional 500 mL of the feedstock was fed to the reactor to test the reusability of the enzymes and the yeast bed as well as the continuous operability of the system. Again, when the feedstock was completely fed to the reactor, DDW was streamed through in order to convert the

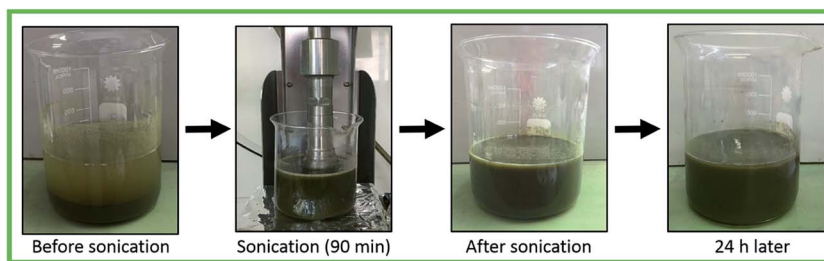


Fig. 11 The aqueous suspension of *Ulva rigida* (5 wt%) before and after the sonication process.⁵⁸

residual carbohydrate content of the algae to bioethanol. The experimental setup of the continuous-flow SSF process of the marine macroalgae *Ulva rigida* in the solar reactor is presented in Fig. 12. It is important to note that similar bioethanol results were obtained when the same experiment was repeated by loading the enzymes and baker's yeast on activated carbon prior to the SSF process.⁵⁸

The SSF process of 5 wt% *Ulva rigida* was monitored for 37 days in the solar reactor (with the same enzymes and yeast) at an average day/night temperature of 31/24 °C. The aliquots of the products were collected at regular time intervals and quantified for ethanol using ¹H NMR spectroscopy and HPLC. The ethanol yield (deduced from ¹H NMR analysis) as a function of time is depicted in Fig. 13. High ethanol yields (84% of the theoretical ethanol yield with green chemistry metrics RME = 15% and MI = 0.84) were observed throughout the SSF process of *Ulva rigida* (0.2 g ethanol per day, 2.64 g ethanol per day per m²), based on the fermentable sugar content of the biomass (Table 1). As in the SSF of *Ulva rigida* to bioethanol in the batch process, no

peaks other than the characteristic peaks of ethanol were observed in the ¹H and ¹³C NMR spectra of the reaction products of the SSF of *Ulva rigida* in a continuous-flow process.⁵⁸ This indicates that the reaction product is pure aqueous ethanol and is devoid of the reactants (starch and cellulose), reaction intermediate (glucose), and usual secondary metabolites of fermentation (glycerol and acetic acid).

4. Applications of bioethanol produced in the solar reactor

4.1. The potential of bioethanol for application in fuel cells

4.1.1. Fuel cells: a promising energy-conversion device for the future. Fuel cells are efficient energy-conversion (chemical to electrical) devices with low pollutant emission and feedstock flexibility.^{50,63,64} Electricity generation using solar energy and biomass not only reduces the dependence on fossil fuels but also decreases the greenhouse gas emission during power production. Biomass-to-electricity conversion using natural biomass resources can be achieved using fuel-cell technology. Abundant organic raw materials such as alcohols (methanol and ethanol), organic acids (formic acid), and glucose can be used as fuels. Depending on the input fuel and electrolyte, different chemical reactions occur.⁵⁰ Solid oxide fuel cells require high operating temperatures for biomass gasification, whereas microbial fuel cells suffer from the drawbacks of low power output and limited lifetime. The polymer-exchange membrane fuel cell (PEMFC) is

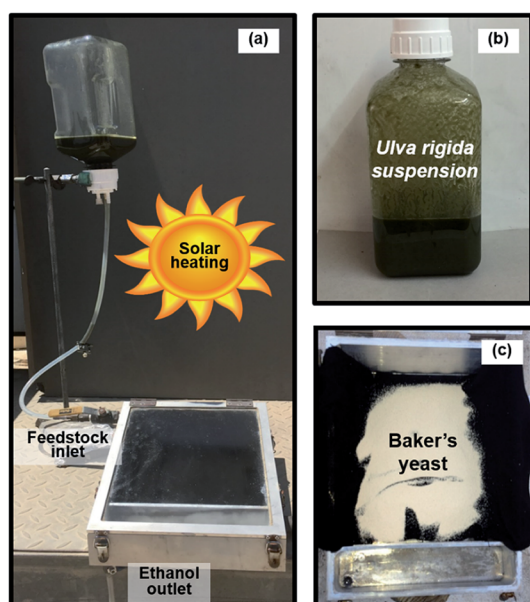


Fig. 12 Continuous-flow solar reactor for the single-step conversion of marine macroalgae *Ulva rigida* to bioethanol; complete experimental setup (a), stable 5 wt% aqueous *Ulva rigida* suspension with enzymes (b), and fermentation chamber loaded with baker's yeast on activated carbon cloth (c).⁵⁸

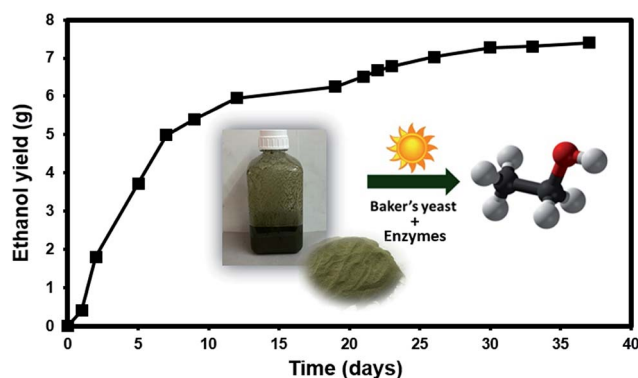


Fig. 13 Time on stream studies of solar-energy-driven bioethanol production in a continuous-flow SSF process of *Ulva rigida* (5 wt%) (T_{ave} day/night: 31/24 °C).⁵⁸

the most practically viable fuel-cell technology. PEMFCs using either hydrogen or low-molecular-weight alcohols (methanol) have been commercialized. However, there is much room for improvement of the fuel, electrode materials, and polymer membrane for the large-scale use of fuel cells for domestic as well as transportation applications.⁶⁵

The direct conversion of biomass to electricity *via* fuel-cell technology is a challenge, as the C–C bonds of biopolymers (starch, cellulose, and lignin) cannot be completely electro-oxidized to CO₂ at low temperatures even with a noble-metal catalyst. Recently, Liu *et al.* developed a photocatalytic (H₃PMo₁₂O₄₀) strategy for the operation of a hybrid fuel cell using biomass (starch, cellulose, lignin, switch grass and wood powders) as fuel. However, the maximum power density of the solar-induced hybrid fuel cell with cellulose as fuel is only 0.72 mW cm⁻².⁶⁶ Tabah *et al.* developed an innovative strategy for improving the power density of the PEMFCs (410 mW cm⁻²) using the bioethanol produced from biomass with the aid of solar energy and subsequently utilizing the bioethanol to power the alkaline-acid direct ethanol fuel cells (AA-DEFCs).^{47,50} Hydrogen produced by the gasification of biomass is also being used as fuel for PEMFC applications, but this is beyond the scope of our review.⁶⁷

4.1.2. Can fuel cells be used for transportation applications? Renewable as well as decentralized (distributed) power supply can be achieved using fuel-cell technology.^{50,64} Due to worldwide efforts over the last decade, the performance of fuel cells with respect to energy efficiency, volumetric and mass power density, and low-temperature startup ability has shown significant progress, leading to the development of fuel-cell technology that is beneficial to the sustainable-transportation sector.^{50,64} Using biomass-to-fuel cell systems, emergency power can be generated for critical operations in the case of power failures lasting for several hours. Direct methanol fuel cells (DMFCs) were used as a substitute for batteries in portable electronic gadgets (mobile phones, MP3 players, computers) for household applications. A significant portion of the energy demand in the transportation sector can also be met by fuel cells. Hydrogen-fueled PEMFCs were used in fuel cell engines (3 kW L⁻¹ power density) by Toyota (Japan) and in an engine module (5 kW L⁻¹ power density) by England Intelligent Energy EC 200-192.^{50,68} Specific advantages of using fuel cells for transportation include negligible emission of CO_x, NO_x and SO_x, operation without noise, and a cold start even at 243 K.^{50,69}

Currently, hydrogen is used as a promising fuel due to its high energy density (32 kW h kg⁻¹). However, it is important to note that the storage and handling of hydrogen are problematic and costly.^{50,69} The fuels that can be alternatives to hydrogen in the production of electricity in a fuel cell include carbon-containing liquids such as bioethanol, methanol, biodiesel, dimethyl esters, and Fischer–Tropsch liquids.⁵⁰ Bioethanol has specific advantages as a promising fuel for fuel cells: (i) ethanol is a good substitute for hydrogen in terms of production, cost, storage, and handling; (ii) the use of bioethanol requires only negligible changes to fuel-cell vehicles and minimal adjustment to the fueling infrastructure; (iii) ethanol ignites at much higher temperatures, resulting in fewer car fires and explosions; (iv)

bioethanol can be produced through the fermentation of renewable sources; (v) ethanol has lower toxicity and higher energy density (8.0 kW h kg⁻¹) than methanol (6.1 kW h kg⁻¹) as well as lower reactivity in the atmosphere, and it contains negligible NO_x, volatile organic compounds, and SO_x; (vi) ethanol does not contain toxic benzene, toluene, ethylbenzene or xylene (BTEX) additives which are found in other fuels as a result of the production process.^{50,70}

DEFCs can be the most promising candidates for portable, mobile, and stationary applications.^{50,71} Recently, various DEFC configurations have been considered (*e.g.* proton-exchange membrane DEFCs, anion-exchange membrane DEFCs, and alkaline-acid DEFCs) and their performance is still being investigated.^{50,72} The basic principle underlying the operation of all DEFCs is the same, and all the cell configurations are under development. A comprehensive review of past research on the development of DEFCs, including catalytic aspects, ion-exchange membranes, and single-cell design and performance, has been reported in recent articles.^{17,50,72–78}

4.2. Starch-based bioethanol as fuel in DEFCs

The bioethanol (1.3 M, 6 wt%) produced in the solar-energy-driven SSF of starch (15 wt%) was tested as a fuel in DEFCs. The purity and potential of the as-produced bioethanol were evaluated by performing electrochemical measurements.^{31,50} Linear sweep voltammograms recorded with a Pt/C (E-TEK) catalyst in 0.5 M H₂SO₄ and 1.3 M ethanol (bioethanol or commercial ethanol) at a scan rate of 25 mV s⁻¹ are shown in Fig. 14a. A typical ethanol oxidation peak appears at +0.75 V. The voltammogram peaks of bioethanol and commercial ethanol are similar, with comparable peak current values (~310 mA mg_{Pt}⁻¹). These features reflect the high purity level of the bioethanol produced by the solar-energy-driven SSF of starch. Single-cell DEFC performance was tested at various temperatures (303, 333 and 363 K) using bioethanol (1.3 M) as fuel, and the corresponding *I*–*V* curves are shown in Fig. 14b. The TEM image, XRD pattern, and EDX spectrum of the commercial Pt/C are shown in Fig. 14c–e. The effect of the temperature on the open-circuit potential (OCP, 0.75 V) is negligible. As expected, an increase in the cell performance was observed with an increase in the operation temperature due to the enhancement of the kinetics of the anodic (ethanol oxidation) and cathodic (oxygen reduction) reactions. Limiting current density values of 116, 155, and 212 mA cm⁻² were observed corresponding to power density values of 25.6, 33.3, and 47.7 mW cm⁻² at operating temperatures of 303, 333, and 363 K, respectively.^{31,50} Thus, the bioethanol produced from starch *via* the solar-energy-driven SSF process is a clean and sustainable potential fuel for DEFCs.

4.3. Glucose-based bioethanol as fuel in AA-DEFCs

Following successful results with the solar-energy-driven SSF of starch, the batch process of bioethanol production was further developed to a continuous-flow process.^{47,50} The bioethanol (2 M, 8.7 wt%) produced from the solar-energy-driven continuous-flow solid-state fermentation of glucose (20 wt%) was tested as a fuel in AA-DEFCs.^{47,50} A schematic representation

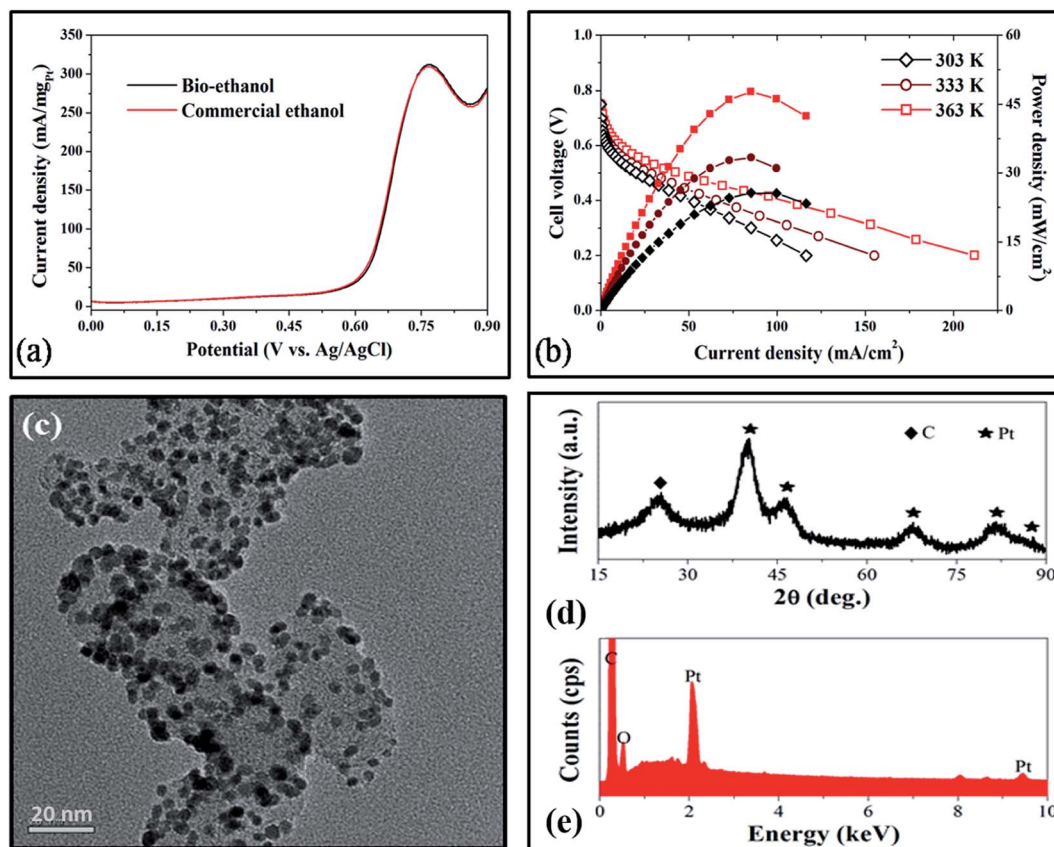


Fig. 14 Linear sweep voltammograms for the electrooxidation of ethanol in 0.5 M H₂SO₄ + 1.3 M C₂H₅OH (Pt/C; scan rate – 25 mV s⁻¹) (a), polarization and power density curves at 2 mg cm⁻² catalyst loading for Pt/C (40 wt%, E-TEK) on both the anode and cathode at different temperatures (anode feed: 1.3 M bioethanol at 1 mL min⁻¹; cathode feed: pure humidified oxygen at 200 mL min⁻¹) (b), TEM (c), XRD (d), and EDX (e) of the commercial Pt/C. Reprinted with permission.³¹ Copyright 2015 John Wiley and Sons, Inc.

of AA-DEFCs is provided in Fig. 15a. The fuel cell comprises alkalized bioethanol (2 M bioethanol + 5 M NaOH) and acidified H₂O₂ (4 M H₂O₂ + 1 M H₂SO₄) compartments separated by a cation-conducting membrane. Bimetallic Pd electrocatalysts, namely, 30 wt% Pd₁Ni₁/C and 50 wt% Pd₁Au₁/C, were used as anode (ethanol oxidation) and cathode (H₂O₂ reduction) electrocatalysts, respectively. Vulcan XC-72 was used as a carbon support in the preparation of the electrocatalysts *via* NaBH₄ reduction. The active-material loading on the anode and cathode was maintained at 1.0 and 3.5 mg cm⁻², respectively. The particle size of the electrocatalysts determined using TEM images is ~5–6 nm (Fig. 15b and c). The 3D-network structure of the electrodes is depicted in the SEM images in Fig. 15d and e. Such a 3D-structured electrode facilitates the diffusion of the reactant species by improving the electrochemically active surface area. At operating temperatures of 303 and 333 K, power density values of 330 and 410 mW cm⁻² were observed, respectively, at a modest open circuit voltage (OCV) of 1.65 V, as shown in the current–voltage (*I*–*V*) polarization and power density curves in Fig. 15f. XRD patterns of Pd₁Ni₁/C and Pd₁Au₁/C catalysts are shown in Fig. 15g.^{47,50}

The OCV and power density values achieved using the AA-DEFC configuration are higher than the values derived using either acid DEFCs or alkaline DEFCs due to the

elimination of the mixed-potential phenomenon.^{50,76–78} The improved performance of the AA-DEFCs as well as the high values of the current and power densities can also be attributed to the high catalytic activity of the bimetallic Pd electrocatalysts comprising the 3D-structural electrode configuration. Specific advantages of using AA-DEFCs include (i) the high power density, (ii) the faster kinetics of ethanol oxidation in alkaline medium, (iii) the faster kinetics of hydrogen peroxide reduction in acidic medium, (iv) the use of non-noble metal electrocatalysts, (v) the low fuel cross-over, (vi) the low activation loss, and (vii) the high theoretical cell voltage (2.52 V).^{50,72,79,80} In conclusion, the bioethanol produced from glucose *via* the solar-energy-driven SSF process is successfully demonstrated as a potential fuel for AA-DEFCs with current and power density values as high as 700 mA cm⁻² and 330 mW cm⁻² at a modest OCV of 1.65 V.³¹ Thus, a new avenue has been explored for a decentralized power supply based on solar energy.

4.4. Comparison of DEFC performances based on ethanol concentration and purity

The purity of bioethanol influences the fuel cell performance and it is anticipated that the purity level should be 99.999% for

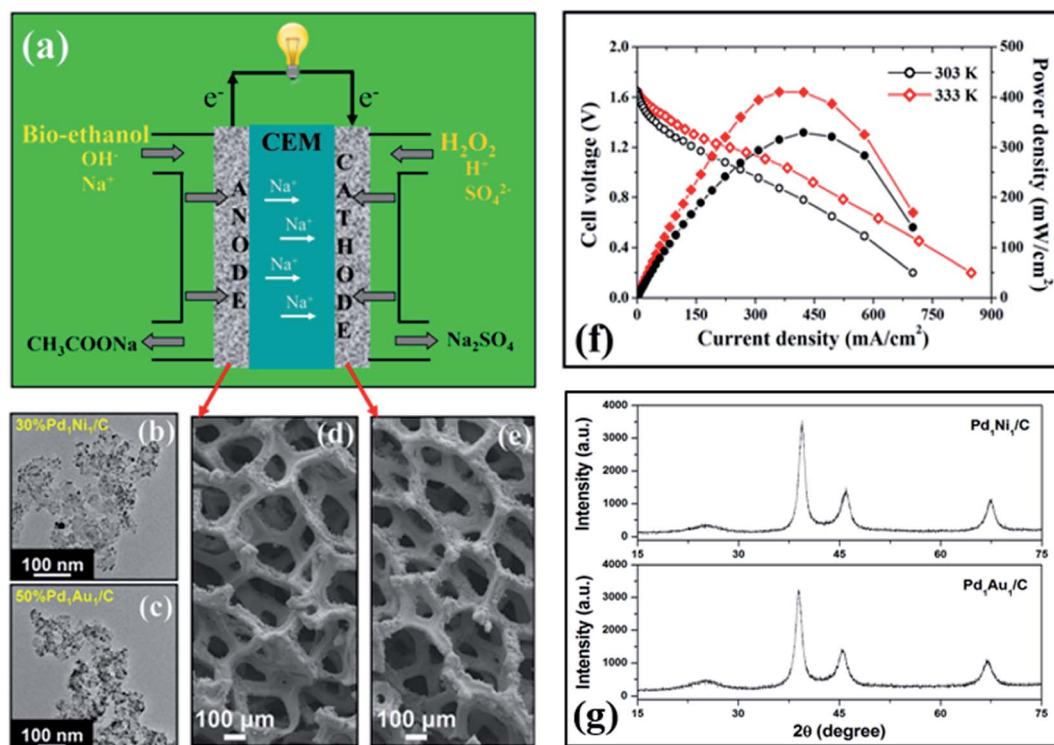


Fig. 15 Schematic depiction of AA-DEFCs (a), TEM images of bimetallic Pd electrocatalysts (b and c), SEM images of the anode and cathode (d and e), current–voltage (I – V) polarization and power density curves (f), and XRD patterns of Pd₁Ni₁/C and Pd₁Au₁/C catalysts (g). Adapted with permission.⁴⁷ Copyright 2016 Royal Society of Chemistry.

successful fuel cell operations. Impurities in bioethanol originate from the raw materials and/or the fermentation process. Possible impurities are methanol, 1-propanol, allyl alcohol, ethyl acetate, diethyl amine, acetic acid, dimethylsulfoxide, dimethyldisulfide, and particulate matter. It has been demonstrated that the impurity level was extremely low when the bioethanol was produced from sugar- and starch-based feedstocks compared to that from wood and straw.⁸¹ Traces of impurities may suppress the DEFC performance by catalyst poisoning and/or preventing the ionic path of the electrolyte. In a recent study, the degradation experiment was conducted by using a single cell and adding nine impurities, namely, methanol, acetaldehyde, acetic acid, 1-propanol, allyl alcohol, ethyl acetate, 3-methyl-1-butanol, acetal (acetaldehyde diethyl acetal), and benzaldehyde to a 2 M aqueous ethanol solution.⁸² The catalyst used for electrooxidation of ethanol was PtRu/C. The relation between the impurity species at specific concentrations and the degradation of the current density was studied. Allyl alcohol, which has a double bond, showed a serious poisoning effect, while the effect of other impurities was negligible at the estimated concentrations in the bioethanol.⁸²

The concentration of ethanol (or water content) is another factor that influences the fuel cell performance. It is generally assumed that 1 to 2 M ethanol is the best option for acid or alkaline DEFCs in terms of performance as well as durability. High concentrations of ethanol can be used to achieve high power density values but durability of fuel cell components is an important issue to be considered. Other factors that influence

the performance are the catalyst, catalyst loading, type of electrolyte/membrane, and temperature.^{72,81,82} We have reviewed and tabulated the studies reported in the literature regarding the effect of ethanol concentration on acid (Table 2) and alkaline (Table 3) DEFC performance (power density). Since we used sugar- and starch-based feedstocks and activated carbon (as the adsorbent) in our solar-energy-driven SSF experiments, we anticipate that the produced bioethanol is of high purity and, therefore, applicable for DEFCs. High current and power density values obtained using our 1.3 M starch-based and 2 M glucose-based bioethanol (reported in Sections 4.2 and 4.3) validate our anticipation, demonstrating a clean and sustainable potential fuel for DEFCs.^{31,47,50}

5. Production of value-added chemicals using solar energy

5.1. *In situ* bioconversion of glycerol to 1,3-propanediol during the solar-energy-driven SSF of starch to ethanol

Glycerol is the inevitable secondary metabolite in the conversion of carbohydrates to bioethanol and lipids to biodiesel. Crude glycerol is rapidly becoming a “waste product” with associated disposal cost due to its production in large quantities in the emerging biofuel industry.^{83,84} The effective utilization of glycerol as a feedstock for the production of value-added products makes the biofuel production processes profitable and environmentally friendly. The production of propanediols

Table 2 Acid DEFC performances

Fuel	Oxidant	Anode	Cathode	Membrane	Temp. (°C)	Power density (mW cm ⁻²)	Ref.
1 M ethanol	2 bar O ₂	Pt ₃ Sn/C	Pt/C	Nafion 117	90	41	103
2 M ethanol	3 bar O ₂	Pt ₈₀ Sn ₂₀ /C	Pt/C	Nafion 117	90	37	104
2 M ethanol	2 atm O ₂	Pt ₆₀ Sn ₄₀ /C	Pt/C	Nafion 117	90	37	105
1.5 M ethanol	0.2 MPa O ₂	PtSn/C–B	Pt/C	Nafion 115	90	82	106
3 M ethanol	1 atm O ₂	PtSn/C	PtCo/C	Nafion 117	90	27.5	107
1 M ethanol	2 atm O ₂	Pt ₂ Sn/C	Pt/C	Nafion 115	90	62	108
2 M ethanol	3 bar O ₂	PtSnIr/C	Pt/C	Nafion 117	90	35	109
1 M ethanol	2 bar O ₂	PtSn/C	Pt/C	Nafion 115	90	55	110
1 M ethanol	3 atm O ₂	PtRu/C	PtSnRu/C	Nafion 115	110	32	111
2 M ethanol	3 bar O ₂	PtSnRu/C	Pt/C	Nafion 117	80	50	112
1 M ethanol	2 atm O ₂	PtRu/C	Pt/C	Nafion 115	75	19.4	113
2 M ethanol	1 bar O ₂	PtRu/C	Pt/C	Nafion 117	80	60	114
1 M ethanol	2 bar O ₂	Pt ₂ Sn/C	Pt/C	Nafion 115	90	52	115
2 M ethanol	1 bar O ₂	Pt ₁₀₀ Sn ₂₀ /C	Pt/C	Nafion 115	90	45	116

Table 3 Alkaline DEFC performances

Fuel	Oxidant	Anode	Cathode	Membrane	Temp. (°C)	Power density (mW cm ⁻²)	Ref.
1 M ethanol + 0.5 M KOH	100 sccm O ₂	PtRu black	Pt black	AEM (A201)	30	58	117
2 M ethanol + 2 M KOH	0.2 MPa O ₂	PtRu/C	Pt/C	PBI/KOH	90	61	118
2 M ethanol + 3 M KOH	O ₂	Pt black	MnO ₂	Teflon	45	55	119
3 M ethanol + 5 M KOH	O ₂	PdNi/C	Acta Hypermec, K14	AEM (A201)	60	90	120
3 M ethanol + 5 M KOH	O ₂	Pd ₃ Au/C	Acta Hypermec, K14	AEM (A201)	40	53	121
3 M ethanol + 5 M NaOH	4 M H ₂ O ₂ + 1 M H ₂ SO ₄	PdNi/C	Pt/C	CEM (Nafion211)	60	360	79
3 M ethanol + 5 M NaOH	O ₂	PdNi/C	Acta Hypermec, K14	CEM (Nafion211)	90	135	80
3 M ethanol + 5 M NaOH	4 M H ₂ O ₂ + 1 M H ₂ SO ₄	PdNi/C	Pt/C	CEM (Nafion211)	60	240	122
3 M ethanol + 5 M NaOH	4 M H ₂ O ₂ + 1 M H ₂ SO ₄	PdNi/C	Au/Ni–Cr	CEM (Nafion211)	60	200	123
2 M ethanol + 2 M KOH	Air	PtRu/C	MnO ₂ /C	PBI/KOH	60	30	124
2 M ethanol + 2 M KOH	0.2 MPa O ₂	PtRu/C	Pt/C	CEM (Nafion112)	90	59	125
3 M ethanol + 5 M KOH	O ₂	PdNi/C	Acta Hypermec, K14	AEM (A201)	80	130	126
1 M ethanol + 0.5 M NaOH	O ₂	PtPd–PNVC–V ₂ O ₅	Pt/C	AEM (A201)	40	30	127

through the selective hydrogenolysis of glycerol is a promising strategy for glycerol utilization.^{83,85} 1,3-Propanediol (1,3-PDO) has recently attracted attention as a high-value specialty chemical used primarily in the preparation of polyester fibers, films, and coatings.⁸⁶ In 2012, the global demand for 1,3-PDO was 60.2 kt, with a market value of \$2.61 per kg.⁸⁷ By 2019, the demand is expected to reach 150 kt and the price is estimated to increase to \$3.73 per kg.⁸⁷ The high price of 1,3-PDO indicates the economic sustainability of the glycerol conversion process (pure glycerol: \$0.66 per kg; crude glycerol: \$0.11 per kg).⁸⁷

Tabah *et al.* reported, for the first time, the potential of baker's yeast to convert glycerol to 1,3-PDO, while studying the SSF of starch to bioethanol in the solar reactor.³¹ To monitor the reaction intermediates and byproducts of the SSF of starch, analytes from the fermentation broth were collected from the solar reactor on the 7th and 60th days of the process. The corresponding ¹³C NMR spectra are depicted in Fig. 16. In the analyte from the 7th day, signals typical of glucose, ethanol, and glycerol were observed (Fig. 16a). Glucose is the reaction intermediate of the SSF process, formed from the saccharification of

starch by the action of amylases. Likewise, bioethanol is the major reaction product and glycerol is the byproduct of the fermentation of glucose to ethanol.

In contrast, the analyte from the broth collected on the 60th day shows no trace of glycerol. Rather, signals typical of 1,3-PDO, a hydrogenolysis product of glycerol, can be seen in the ¹³C NMR spectrum (Fig. 16b). In addition, no signals corresponding to glucose were observed on the 60th day, as all the glucose was converted to the product bioethanol, indicating the completion of the SSF of starch to bioethanol. Thus, the value-added product 1,3-PDO was formed by the *in situ* bioreduction of glycerol.³¹

Due to the increased demand for 1,3-PDO-based polymers, the process of bioreduction of glycerol to 1,3-PDO was further studied under various fermentation conditions (aerobic, semi-aerobic and anaerobic) at different reaction temperatures (25–37 °C) to optimize the process and the yield of 1,3-PDO. Aliquots collected at regular time intervals were analyzed both qualitatively (¹³C NMR) and quantitatively (HPLC).⁸³ The yields (wt%) of the target product 1,3-PDO and other metabolites in the

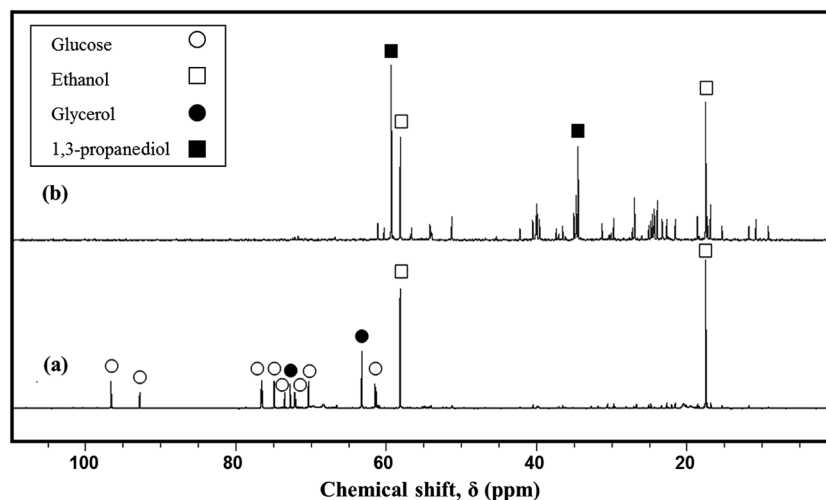


Fig. 16 ^{13}C NMR spectra of the samples collected from the broth on the 7th (a) and 60th (b) day of the SSF of starch (5 wt%) in the solar reactor. Reprinted with permission.³¹ Copyright 2015 John Wiley and Sons, Inc.

samples collected from the reaction medium on the 30th day are summarized in the form of a histogram (Fig. 17). It is interesting to note from the HPLC analysis that the glycerol fermentation products consist of different metabolites such as ethanol, acetic acid, lactic acid, propionic acid, and formic acid, in addition to the desired product 1,3-PDO. Anaerobic fermentation of glycerol at 25 °C was found to be the optimal reaction condition, resulting in 93.6 wt% glycerol conversion and 42.3 wt% yield of 1,3-PDO (Fig. 17A).⁸³

The reaction temperature and the extent of availability of oxygen (fermentation type) are the crucial parameters directing the metabolic pathway of the yeast (*S. cerevisiae*) during the glycerol fermentation. Under aerobic fermentation and the lowest reaction temperature studied (25 °C), the yield of 1,3-PDO was the highest (42.3 wt%) and the formation of propionic acid (<1 wt%) was the least (Fig. 17A). In contrast, when glycerol fermentation is carried out under semi-aerobic conditions (at 25 °C) where the availability of oxygen is greater, the propionic acid pathway is preferred (42.4 wt% yield) over the 1,3-PDO (9.9 wt%) (Fig. 17A). Under aerobic conditions where there is no restriction on oxygen flow, the yeast has no preferential pathway, as evident from the nearly equal yields of 1,3-PDO (25.4 wt%) and propionic acid (21.7 wt%). In contrast, the aerobic fermentation of glycerol at higher reaction temperatures (either 30 or 37 °C) is detrimental to the 1,3-PDO pathway (yield, <2 wt%) (Fig. 17B and C).⁸³

The ability of *S. cerevisiae* to directly metabolize glycerol and convert it to 1,3-PDO is a significant finding and offers a promising alternative pathway to the traditional methods that use non-renewable fossil resources as feedstocks for the production of 1,3-PDO. Synthesizing 1,3-PDO by biological means is extremely important, because it is comparatively more environment-friendly than chemical conversion and, from an economical perspective, is generally more advantageous, since milder conditions are used, less energy is required, and greater yields are attainable for specific products.^{83,86,88,89}

5.2. Production of 1,3-PDO and other secondary metabolites during the solar-energy-driven SSF of *Ulva rigida* to ethanol

Aliquots collected at regular time intervals from the solar-energy-driven batch and continuous-flow fermentation broth of *Ulva rigida* were analyzed both qualitatively (^{13}C NMR) and quantitatively (HPLC).⁵⁸ In addition to the target product ethanol, other metabolites such as 1,3-PDO, glycerol, acetic acid, and lactic acid were also observed in the fermentation broth. These secondary metabolites cannot be evaporated due to their low vapor pressures compared to bioethanol; therefore, they remained in the fermentation broth, yet did not affect the catalytic activity of the microorganisms. The concentration of the metabolites in the samples collected at regular time intervals from the reaction medium is summarized (from the HPLC analysis) in the form of a histogram in Fig. 18. At the end of the continuous-flow SSF process of 5 wt% *Ulva rigida* (35th day), 25 mM 1,3-PDO, 16 mM glycerol, 40 mM acetic acid, and 240 mM lactic acid were observed in the fermentation broth in addition to 1.5 mM ethanol (Fig. 18A). Similarly, at the end of the batch SSF process of 10 wt% *Ulva rigida* (55th day), 33 mM 1,3-PDO, 50 mM glycerol, 59 mM acetic acid, 174 mM lactic acid, and 1.8 mM ethanol were observed in the fermentation broth (Fig. 18B).⁵⁸ The concentration distribution of the metabolites observed in the fermentation broth of *Ulva rigida* is quite different from that in the usual fermentations of glucose, starch or cellulose, where the major secondary metabolites are either glycerol or acetic acid. In contrast, in the current study, the major secondary metabolite was observed to be lactic acid with smaller concentrations of acetic acid and glycerol. Under anaerobic conditions at lower pH (4.5), *S. cerevisiae* is known to produce lactic acid from glucose metabolism via the lactate pathway.⁹⁰ Lactic acid may have also been produced from possible chemical catalytic conversions of glucose under the anaerobic conditions prevailing in the solar reactor at 20–35 °C. With marine algae as the feedstock, traces of Na^+ species

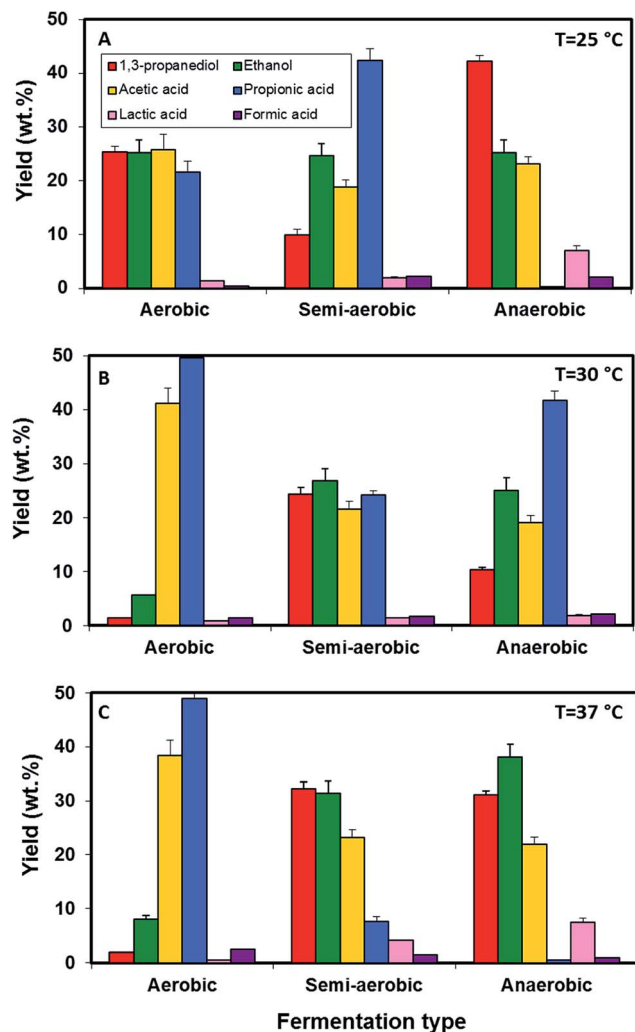


Fig. 17 Yield (wt.%) of 1,3-propanediol and other metabolites (ethanol, acetic acid, lactic acid, propionic acid, and formic acid) through fermentation (aerobic, semi-aerobic and anaerobic) of glycerol (0.1 M) by *S. cerevisiae* (3 g) at 25 (A), 30 (B), and 37 (C) °C on the 30th day. Reprinted with permission.⁸⁵ Copyright 2016 Royal Society of Chemistry.

chemisorbed in the algae might have caused the *in situ* formation of NaOH, which could have catalyzed the conversion of glucose to lactic acid. In fact, Li *et al.* have reported the catalytic activity of NaOH for the conversion of glucose to lactic acid (40% yield) under anaerobic conditions at 25 °C.⁹¹ Another important result of the solar-energy-driven SSF of *Ulva rigida* is the formation of the secondary metabolite 1,3-PDO by the *in situ* bioconversion of glycerol, which was first demonstrated by our group during the SSF of starch to bioethanol.^{31,50,58}

The metabolites in the fermentation broth were further determined qualitatively by ¹³C NMR analysis. The analytes from the broth confirm the results deduced from HPLC analysis and show the presence of organic acids (acetic and lactic), glycerol, and 1,3-PDO in addition to the desired product ethanol, as indicated in the ¹³C NMR spectrum in Fig. 19.⁵⁸

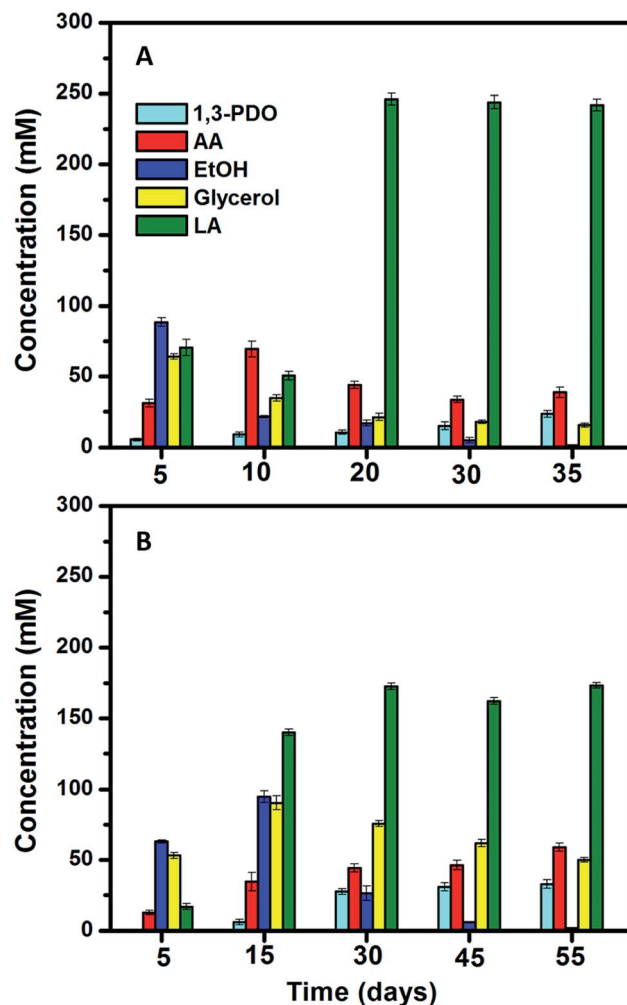


Fig. 18 Concentration of metabolites in the fermentation broth of solar-energy-driven bioethanol production from 5 wt% (continuous flow) (A) and 10 wt% (batch) (B) *Ulva rigida* suspension as a function of time.⁵⁸

6. Utilization of solar energy for the upcoming biorefinery

Intensive research is being carried out on the conversion of biomass into chemicals, biofuels, and various other materials, with the prospect to create new “biorefinery” processes needed for future economies.^{50,92} The development of biorefineries that utilize free renewable, abundant, solar thermal energy can create remarkable opportunities for the forestry, biotechnology, materials, and chemical processing industries, as well as stimulate advances in agriculture. It can eventually help create a sustainable society and industries that use renewable and carbon-neutral resources.⁵⁰

6.1. Future prospects of bioethanol production in solar reactors

Future efforts will focus on upscaling the present solar-energy-driven process for biofuel and biochemical production in two

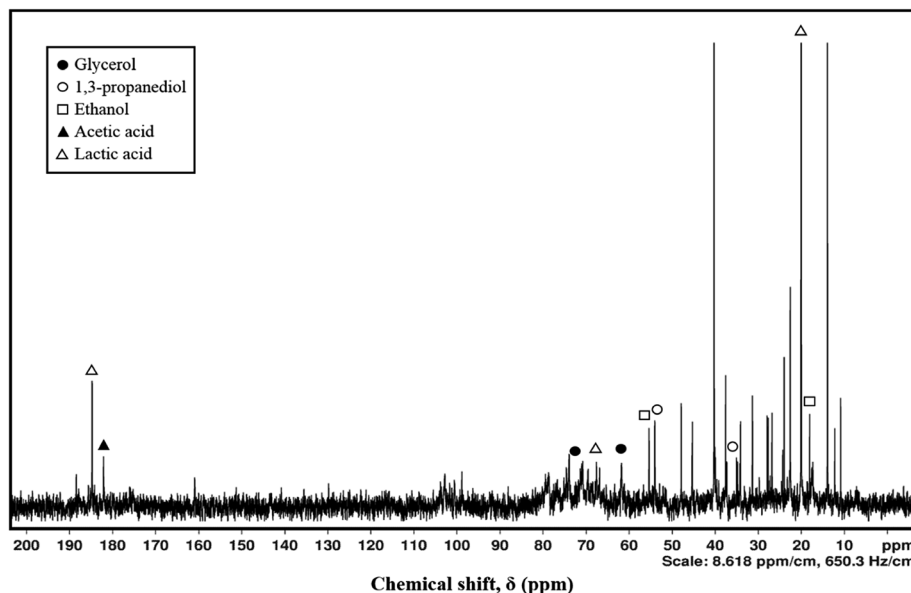


Fig. 19 ^{13}C NMR spectrum of metabolites from fermentation broth (day 35) of solar-energy-driven bioethanol production from the continuous-flow SSF process of 5 wt% *Ulva rigida*.⁵⁸

stages.⁵⁰ In the first stage, the size of the current solar reactor can be increased by a factor of four, resulting in volume enhancement by a factor of 64. The new dimensions can enable an increase in the flow rate of the feedstock, also by a factor of four. In the second stage, the design of the solar reactor can be further improved. In this stage, in addition to the change in dimensions, the design of the solar reactor can be further modified into a stair-case structure. Such an upscaling can enhance the reactor volume by a factor of 360, enabling the handling of large quantities of biomass feed for the demand-based supply of bioethanol for transportation and chemical industry applications. Therefore, any progress in this direction will open new avenues towards sustainable biorefinery. The target of this prototype is to convert 10 kg of feedstock per day.

6.2. Using solar-energy-based bioethanol to produce valuable chemicals

The bioethanol produced from the SSF of biomass (marine and freshwater algae, lignocellulosic materials) can form a sustainable feedstock for the synthesis of value-added chemicals such as diethyl ether (DEE) and ethylene. DEE is a potential transportation fuel, while ethylene is a promising feedstock for a variety of polymers.^{50,93,94} The production of value-added chemicals from bioethanol generated *via* solar-energy-based processes not only reduces reliance on fossil resources but also makes the chemical-production processes energy-efficient and competitive. Apart from bioethanol, the synthesis of valuable fuels such as formic acid can also be attempted from glucose oxidation driven by solar energy. Formic acid is an ideal hydrogen storage material, and efforts should be devoted to the development of sustainable processes for the selective conversion of biomass to formic acid.⁹⁵

6.3. Role of novel materials in the solar-energy-driven conversion of biomass to biofuels

Although bioethanol is a promising transportation fuel, the process of glucose fermentation has an inherent limitation of 51% theoretical process efficiency. This is due to the fact that a maximum of 0.51 g of bioethanol can be produced from 1 g of glucose, while the remainder becomes CO_2 .^{47,48} There is a great need to improve the atom efficiency of the glucose fermentation process. Attempts should be made to perform the SSF process of biomass in the solar reactor in the presence of additional microorganisms which may *in situ* metabolize the CO_2 evolved during the fermentation reaction. Such a strategy may further improve the process efficiency.⁹⁶ Moreover, novel materials based on graphene, which have high potential for photo-absorption, can be very useful.^{97,98}

Recently, unconventional materials such as millimetric silica beads and waste polyethylene films have been used for the deposition of nanoparticles of catalysts (SrO) and biocatalysts (pepsin) *via* sonication.^{99,100} Such catalytic systems outperform the native catalysts (SrO or pepsin). Moreover, the use of such heterogeneous catalytic systems has both economic and environmental benefits. The simultaneous co-deposition of enzymes (amylases and cellulases) and yeast on unconventional supports such as millimetric silica beads/polyethylene films can result in the formation of nanoparticles of the biocatalytic species, exhibiting improved performance for the conversion of biomass into bioethanol in a solar-energy-driven SSF process. Thus, a wide variety of novel materials can be used to improve the process efficiency of biofuel production. To reach this goal, intense research is needed in the near future. The use of these new materials can play a promising role in accelerating the solar-energy-driven SSF process, as well as enhancing the rate of

the evaporation and condensation process, with the net result of improving the bioethanol productivity.

In addition, the evaluation and economic optimization of SSF for ethanol production require knowledge of the chemical and biological processes involved. Although the SSF process is being investigated extensively, there are still no guidelines for the optimal conditions for the SSF of various feedstocks, such as softwoods (*e.g.*, pine and spruce).¹⁰¹ Since softwoods are more resistant to hydrolysis, they are more difficult to utilize as feedstock than hardwoods (*e.g.* oak, aspen, and poplar).¹⁰² Future studies should focus on combining the existing fermentation techniques with the novel materials that can make the solar-energy-driven biofuel production sustainable and industrially competitive.

7. Conclusions

Successful utilization of solar energy for bioethanol production from biomass has potential to improve the fuel shortage problem. In the current study, the solar energy was used as a heating element for the catalyst and the reaction volume, replacing an oven or heating plate. In the same way, the extraction step was also aided by this heating element. The ethanol produced in the reactor was separated from the fermentation broth soon after its formation by an evaporation–condensation process. Although solar energy is unstable in terms of limited day hours and seasons, the present study demonstrates the operability and the sustainability of the process even in the winter season with lower temperatures (~20 °C). Thus, a new avenue was explored for decentralized power supply based on solar energy.

There is no similar or parallel system operating on these principles in the literature. Such application is first of its kind and could be regarded as a breakthrough and prelude to several other applications in chemical industries and the transportation sector. From the green chemistry point of view, the solar-energy-driven SSF process has numerous advantages. The reaction time is short, due to the coupling of the hydrolysis and fermentation stages into one stage. The SSF process is more economical because both the hydrolysis and fermentation stages are performed in the same reactor. High ethanol yields were obtained (up to 91% of the theoretical yield) by performing various solar-energy-driven fermentation reactions indicating the atom efficiency of the process. No traces of the reactant or secondary metabolites were observed in the product; therefore the product was only aqueous ethanol.

The superior features of the current approach for bioethanol production are (i) the bioethanol production process is a continuous flow which could be easily adopted for industrial applications for large scale production, (ii) it uses solar thermal energy for fermentation and separation of the formed ethanol, (iii) it achieves high ethanol yields without electricity consumption (no external source of heating), making the whole process green, sustainable, and most importantly cost effective, (iv) it uses the same microorganism (without any additional nutrients) and enzymes for a long time (at least two months) without loss in the activity, (v) no polluting effluent is produced

during the process, (vi) it demonstrates the potential of the produced bioethanol as fuel in DEFCs, and (vii) this economically feasible and environment-friendly process was also demonstrated for *in situ* production of a value-added chemical 1,3-PDO from the secondary metabolite of glucose fermentation, glycerol. The current methodology of bioethanol production is applicable to various biomass and feedstock containing glucose, starch, and/or cellulose (such as agricultural crops and residues, cellulosic and lignocellulosic biomass, dry and wet wastes, and marine and freshwater algae).

Acknowledgements

The authors acknowledge the financial support from the Israel Science Foundation (ISF, Grant No. 598/12), from the Ministry of Science, Technology, and Space of Israel (Grant No. 3-9802 and 3-99763), and from the Israel Ministry of National Infrastructures, Energy and Water Resources (Grant No. 3-13442). The authors thank Mr Menachem Schneeberg, head of mechanical workshop at Bar-Ilan University, for fabricating the solar reactor. The authors are also grateful to Dr Hugo Gottlieb, head of the NMR unit at Bar-Ilan University, for fruitful discussions on NMR analysis.

References

- 1 S. P. Singh and D. Singh, *Renewable Sustainable Energy Rev.*, 2010, **14**, 200–216.
- 2 M. Schmidt, M. Porcar, V. Schachter, A. Danchin and I. Mahmutoglu, Biofuels, in *Synthetic Biology: Industrial and Environmental Applications*, ed. M. Schmidt, Wiley-VCH Verlag GmbH & Co. KGaA, Weinheim, Germany, 2012, ch. 1, pp. 7–67.
- 3 I. N. Pulidindi and A. Gedanken, Employing Novel Techniques (Microwave and Sonochemistry) in the Synthesis of Biodiesel and Bioethanol, in *Production of Biofuels and Chemicals with Ultrasound*, ed. Z. Fang Jr, R. L. Smith and X. Qi, Springer, Dordrecht, 2015, vol. 4, The Biofuels and Biorefineries Series, ch. 6, pp. 159–185.
- 4 S. R. Tewfik, N. M. El Defrawy and M. H. Sorour, *Egypt. J. Pet.*, 2013, **22**, 269–276.
- 5 A. Avami, *Renewable Sustainable Energy Rev.*, 2013, **26**, 761–768.
- 6 M. J. Climent, A. Corma and S. Iborra, *Green Chem.*, 2014, **16**, 516–547.
- 7 W. Zhang, Y. Lin, Q. Zhang, X. Wang, D. Wu and H. Kong, *Fuel*, 2013, **112**, 331–337.
- 8 Y. H. P. Zhang, *Process Biochem.*, 2011, **46**, 2091–2110.
- 9 J. E. Anderson, D. M. DiCicco, J. M. Ginder, U. Kramer, T. G. Leone, H. E. Raney-Pablo and T. J. Wallington, *Fuel*, 2012, **97**, 585–594.
- 10 T. Hasunuma and A. Kondo, *Biotechnol. Adv.*, 2012, **30**, 1207–1218.
- 11 S. Nikolić, L. Mojović, M. Rakin, D. Pejin and J. Pejin, *Food Chem.*, 2010, **122**, 216–222.
- 12 P. Subhedhar and P. R. Gogate, *Ind. Eng. Chem. Res.*, 2013, **52**, 11816–11828.

- 13 F. Talebnia, D. Karakashev and I. Angelidaki, *Bioresour. Technol.*, 2010, **101**, 4744–4753.
- 14 D. J. Hayes, S. Fitzpatrick, M. H. B. Hayes and J. R. H. Ross, The Biofine Process-Production of Levulinic Acid, Furfural, and Formic Acid from Lignocellulosic Feedstocks, in *Biorefineries-Industrial Processes and Products: Status Quo and Future Directions*, ed. B. Kamm, P. R. Gruber and M. Kamm, Wiley-VCH Verlag GmbH, Weinheim, Germany, 2005, vol. 1, ch. 7, pp. 139–164.
- 15 H. Su, G. Xu, H. Chen and Y. Xu, *ACS Sustainable Chem. Eng.*, 2015, **3**, 2002–2011.
- 16 I. Farida, K. Syamsu and M. Rahayuningsih, *Int. J. Renewable Energy Dev.*, 2015, **4**, 25–31.
- 17 E. Antolini, *J. Power Sources*, 2007, **170**, 1–12.
- 18 R. H. Petrucci, F. G. Herring, J. D. Madura and C. Bissonnette, Thermochemistry, in *General Chemistry: Principles and Modern Applications*, Pearson Canada Inc., Toronto, Ontario, 10th edn, 2011, ch. 7, pp. 275–280.
- 19 M. S. Elshahed, *J. Adv. Res.*, 2010, **1**, 103–111.
- 20 Y. Lin and S. Tanaka, *Appl. Microbiol. Biotechnol.*, 2006, **69**, 627–642.
- 21 F. W. Bai, *Biotechnol. Adv.*, 2008, **26**, 89–105.
- 22 R. Jevtić-Mučibabić, J. Dodić, J. Ranković, S. Dodić, S. Popov and Z. Zavargo, *Food Feed Res.*, 2008, **35**, 71–76.
- 23 G. Zhao, M. Zheng, J. Zhang, A. Wang and T. Zhang, *Ind. Eng. Chem. Res.*, 2013, **52**, 9566–9572.
- 24 M. F. Chagas, R. O. Bordonal, O. Cavalett, J. L. N. Carvalho, A. Bonomi and N. La Scala Jr, *Biofuels, Bioprod. Biorefin.*, 2016, **10**, 89–106.
- 25 G. Francesca, F. Magherini, T. Gamberi, M. Borro, M. Simmaco and A. Modesti, *Biochim. Biophys. Acta, Proteins Proteomics*, 2010, **1804**, 1516–1525.
- 26 M. Akinori, I. Hiroyuki, K. Tsutomu and S. Shigeki, *Appl. Microbiol. Biotechnol.*, 2009, **84**, 37–53.
- 27 V. B. Kumar, I. N. Pulidindi and A. Gedanken, *Renewable Energy*, 2015, **78**, 141–145.
- 28 R. Anuradha, A. K. Suresh and K. V. Venkatesh, *Process Biochem.*, 1999, **35**, 367–375.
- 29 N. Bozic, M. S. Slavic, A. Gavrilovic and Z. Vujcic, *Bioproc. Biosyst. Eng.*, 2014, **37**, 1353–1360.
- 30 R. Tabassum, S. Khaliq, M. I. Rajoka and F. Agblevor, *Biotechnol. Res. Int.*, 2014, **2014**, 495384.
- 31 B. Tabah, I. N. Pulidindi, V. R. Chitturi, L. M. R. Arava and A. Gedanken, *ChemSusChem*, 2015, **8**, 3497–3503.
- 32 M. Ballesteros, J. M. Oliva, M. J. Negro, P. Manzanares and I. Ballesteros, *Process Biochem.*, 2004, **39**, 1843–1848.
- 33 L. Korzen, I. N. Pulidindi, A. Israel, A. Abelson and A. Gedanken, *RSC Adv.*, 2015, **5**, 16223–16229.
- 34 L. Korzen, I. N. Pulidindi, A. Israel, A. Abelson and A. Gedanken, *RSC Adv.*, 2015, **5**, 59251–59256.
- 35 C. E. Wyman and N. D. Hinman, *Appl. Biochem. Biotechnol.*, 1990, **24**, 735–753.
- 36 M. J. E. C. Van der Maarel, B. Van der Veen, J. C. M. Uitdehaag, H. Leemhuis and L. Dijkhuizen, *J. Biotechnol.*, 2002, **94**, 137–155.
- 37 C. E. Wyman, *Bioresour. Technol.*, 1994, **50**, 3–15.
- 38 F. A. Goncalves, H. A. Ruiz, C. C. Nogueira, E. S. Santos, J. A. Teixeira and G. R. Macedo, *Fuel*, 2014, **131**, 66–76.
- 39 A. Victor, I. N. Pulidindi, T. H. Kim and A. Gedanken, *RSC Adv.*, 2016, **6**, 31–38.
- 40 M. Tampier, D. Smith, E. Bibeau and P. A. Beauchemin, *Identifying environmentally preferable uses for biomass resources*, Envirochem Services Inc., North Vancouver, Canada, Stage I Report: Identification of feedstock-to-product threads, 2004.
- 41 O. Tzhayik, I. N. Pulidindi and A. Gedanken, *Ind. Eng. Chem. Res.*, 2014, **53**, 13871–13880.
- 42 I. N. Pulidindi, B. B. Kimchi and A. Gedanken, *Renewable Energy*, 2014, **71**, 77–80.
- 43 V. B. Kumar, I. N. Pulidindi, Y. Kinel-Tahan, Y. Yehoshua and A. Gedanken, *Energy Fuels*, 2016, **30**, 3161–3166.
- 44 A. Demirbas and F. M. Demirbas, *Energ. Convers. Manage.*, 2011, **52**, 163–170.
- 45 I. N. Pulidindi, L. Korzen, B. Tabah, A. Victor, A. Israel, A. Abelson and A. Gedanken, Potential Applications of *Ulva rigida* for Biofuel and Biochemical Production, in *Seaweeds: Biodiversity, Environmental Chemistry and Ecological Impacts*, ed. P. Newton, Nova Science Publishers Inc., New York, 2017, ch. 3.
- 46 G. G. Satpati and R. Pal, *J. Algal Biomass Utln.*, 2011, **2**, 10–13.
- 47 B. Tabah, I. N. Pulidindi, V. R. Chitturi, L. M. R. Arava and A. Gedanken, *RSC Adv.*, 2016, **6**, 24203–24209.
- 48 B. Tabah, I. N. Pulidindi and A. Gedanken, *J. Bioprocess. Biotech.*, 2015, **5**, 232.
- 49 I. N. Pulidindi, A. Gedanken, R. Schwarz and E. Sendersky, *Energy Fuels*, 2012, **26**, 2352–2356.
- 50 B. Tabah, I. N. Pulidindi, V. R. Chitturi, L. M. R. Arava and A. Gedanken, Solar-energy driven bioethanol production from carbohydrates for transportation applications, in *Solar Energy and Solar Panels: Systems, Performance and Recent Developments*, ed. J. G. Carter, Nova Science Publishers Inc., New York, Energy Science, Engineering and Technology Series, 2017, ch. 1, pp. 1–66.
- 51 M. Koberg and A. Gedanken, *Energy Environ. Sci.*, 2012, **5**, 7460–7469.
- 52 M. Topf, M. Koberg, Y. Kinel-Tahan, A. Gedanken, Z. Dubinsky and Y. Yehoshua, *Biofuels*, 2014, **5**, 405–413.
- 53 G. Corro, N. Sanchez, U. Pal and F. Banuelos, *Waste Manage.*, 2016, **47**, 105–113.
- 54 M. Zanotti, Z. Ruan, M. Bustamente, Y. Liu and W. Liao, *Green Chem.*, 2016, **18**, 5059–5068.
- 55 J. Whitmarsh and Govindjee, The photosynthetic process, in *Concepts in Photobiology: Photosynthesis and Photomorphogenesis*, ed. G. S. Singhal, G. Renger, S. K. Sopory, K.-D. Irrgang and Govindjee, Narosa Publishers, New Delhi, India, 1999, ch. 2, pp. 11–51.
- 56 N. A. Lange, *Handbook of Chemistry*, McGraw-Hill, New York, NY, 10th edn, 1967, pp. 1522–1524.
- 57 A. Baum, J. Agger, A. S. Meyer, M. Egebo and J. D. Mikkelsen, *New Biotechnol.*, 2012, **29**, 293–301.
- 58 A. Gedanken, I. N. Pulidindi and B. Tabah, U.S. Provisional Pat. Ser. No., 62/450,107, filed on January 25 2017.

- 59 A. Pandey, *Biochem. Eng. J.*, 2003, **13**, 81–84.
- 60 A. I. Galaction, A. M. Lupasteanu and D. Cascaval, *Open Sys. Biol. J.*, 2010, **3**, 9–20.
- 61 C. M. Neves, J. F. Granjo, M. G. Freire, A. Robertson, N. M. Oliveira and J. A. Coutinho, *Green Chem.*, 2011, **13**, 1517–1526.
- 62 J. Baeyens, Q. Kang, L. Appels, R. Dewil, Y. Lv and T. Tan, *Prog. Energy Combust. Sci.*, 2015, **47**, 60–88.
- 63 W. Vielstich, *Fuel Cells: Modern Process for the Electrochemical Production of Energy*, Wiley-Interscience, London, 1st edn, 1965.
- 64 K. Kordesch and G. Simader, *Fuel Cells and Their Applications*, VCH Verlag GmbH, Weinheim, 1st edn, 1996.
- 65 A. V. Prakash, P. Indra Neel and B. Viswanathan, *Indian J. Chem., Sect. A: Inorg., Bio-inorg., Phys., Theor. Anal. Chem.*, 2010, **49**, 1441–1443.
- 66 W. Liu, W. Mu, M. Liu, X. Zhang, H. Cai and Y. Deng, *Nat. Commun.*, 2014, **5**, 3208.
- 67 B. Chutichai, S. Authayanun, S. Assabumrungrat and A. Arpornwichanop, *Energy*, 2013, **55**, 98–106.
- 68 J. Q. Li, C. Fang and L. F. Xu, *J. Automot. Saf. Energy*, 2014, **5**, 17–29.
- 69 P. Preuster, C. Papp and P. Wasserscheid, *Acc. Chem. Res.*, 2017, **50**, 74–85.
- 70 S. Q. Song and P. Tsiakaras, *Appl. Catal., B*, 2006, **63**, 187–193.
- 71 M. Z. F. Kamarudin, S. K. Kamarudin, M. S. Masdar and W. R. W. Daud, *Int. J. Hydrogen Energy*, 2013, **38**, 9438–9453.
- 72 L. An, T. S. Zhao and Y. S. Li, *Renewable Sustainable Energy Rev.*, 2015, **50**, 1462–1468.
- 73 S. Q. Song, W. J. Zhou, Z. H. Zhou, L. H. Jiang, G. Q. Sun, Q. Xin, V. Leonditis, S. Kontou and P. Tsiakaras, *Int. J. Hydrogen Energy*, 2005, **30**, 995–1001.
- 74 W. J. Zhou, W. Z. Li, S. Q. Song, Z. H. Zhou, L. H. Jiang, G. Q. Sun, Q. Xin, K. Pouliantis, S. Kontou and P. Tsiakaras, *J. Power Sources*, 2004, **131**, 217–223.
- 75 J. R. Varcoe and R. C. T. Slade, *Fuel Cells*, 2005, **5**, 187–200.
- 76 A. Brouzgou, A. Podias and P. Tsiakaras, *J. Appl. Electrochem.*, 2013, **43**, 119–136.
- 77 V. R. Chitturi and B. Viswanathan, *J. Phys. Chem. C*, 2009, **113**, 18907–18913.
- 78 V. R. Chitturi and B. Viswanathan, *Electrochim. Acta*, 2010, **55**, 3002–3007.
- 79 L. An and T. S. Zhao, *Int. J. Hydrogen Energy*, 2011, **36**, 9994–9999.
- 80 L. An and T. S. Zhao, *Energy Environ. Sci.*, 2011, **4**, 2213–2217.
- 81 H. Habe, T. Shinbo, T. Yamamoto, S. Sato, H. Shimada and K. Sakaki, *J. Jpn. Pet. Inst.*, 2013, **56**, 414–422.
- 82 H. Ishitobi, D. Naito, Y. Ino, M. Yajima and N. Nakagawa, *J. Jpn. Inst. Energy*, 2016, **95**, 909–914.
- 83 B. Tabah, A. Varvak, I. N. Pulidindi, E. Foran, E. Banin and A. Gedanken, *Green Chem.*, 2016, **18**, 4657–4666.
- 84 J. M. Cavaleiro, M. C. M. de Almeida, C. Grandfils and M. M. R. Da Fonseca, *Process Biochem.*, 2009, **44**, 509–515.
- 85 S. S. Priya, V. P. Kumar, M. L. Kantam, S. K. Bhargava and K. V. Chary, *RSC Adv.*, 2014, **4**, 51893–51903.
- 86 G. Kaur, A. K. Srivastava and S. Chand, *Biochem. Eng. J.*, 2012, **64**, 106–118.
- 87 C. S. Lee, M. K. Aroua, W. M. A. W. Daud, P. Cognet, Y. Pères-Lucchese, P.-L. Fabre, O. Reynes and L. Latapie, *Renewable Sustainable Energy Rev.*, 2015, **42**, 963–972.
- 88 S.-A. Jun, C. Moon, C.-H. Kang, S. W. Kong, B.-I. Sang and Y. Um, *Appl. Biochem. Biotechnol.*, 2010, **161**, 491–501.
- 89 R. Dobson, V. Gray and K. Rumbold, *J. Ind. Microbiol. Biotechnol.*, 2012, **39**, 217–226.
- 90 E. Adachi, M. Torigoe, M. Sugiyama, J.-I. Nikawa and K. Shimizu, *J. Ferment. Bioeng.*, 1998, **86**, 284–289.
- 91 L. Li, F. Shen, R. L. Smith and X. Qi, *Green Chem.*, 2017, **19**, 76–81.
- 92 Z. Fang Jr, R. L. Smith and X. Qi, *Production of Biofuels and Chemicals with Ultrasound*, Springer, Dordrecht, vol. 4, The Biofuels and Biorefineries Series, 2015.
- 93 D. Varisli, T. Dogu and G. Dogu, *Chem. Eng. Sci.*, 2007, **62**, 5349–5352.
- 94 T. Kito-Borsa, D. A. Pacas, S. Selim and S. W. Cowley, *Ind. Eng. Chem. Res.*, 1998, **37**, 3366–3374.
- 95 D. Mellmann, P. Sponholz, H. Junge and M. Beller, *Chem. Soc. Rev.*, 2016, **45**, 3954–3988.
- 96 M. Klein, I. N. Pulidindi, N. Perkas and A. Gedanken, *Biomass Bioenergy*, 2015, **76**, 61–68.
- 97 X. Wang, G. Ou, N. Wang and H. Wu, *ACS Appl. Mater. Interfaces*, 2016, **8**, 9194–9199.
- 98 K.-K. Liu, Q. Jiang, S. Tadepalli, R. Raliya, P. Biswas, R. R. Naik and S. Singamaneni, *ACS Appl. Mater. Interfaces*, 2017, **9**, 7675–7681.
- 99 A. Tangy, I. N. Pulidindi and A. Gedanken, *Energy Fuels*, 2016, **30**, 3151–3160.
- 100 D. Meridor and A. Gedanken, *Enzyme Microb. Technol.*, 2014, **67**, 67–76.
- 101 A. Verma, S. Kumar and P. K. Jain, *J. Sci. Res.*, 2011, **55**, 57–63.
- 102 K. Stenberg, M. Bollok, K. Réczey, M. Galbe and G. Zacchi, *Biotechnol. Bioeng.*, 2000, **68**, 204–210.
- 103 S. C. Zignani, V. Baglio, J. J. Linares, G. Monforte, E. R. Gonzalez and A. S. Arico, *Electrochim. Acta*, 2012, **70**, 255–265.
- 104 F. L. S. Purgato, S. Pronier, P. Olivi, A. R. de Andrade, J. M. Leger, G. Tremiliosi-Filho and K. B. Kokoh, *J. Power Sources*, 2012, **198**, 95–99.
- 105 A. O. Neto, R. W. R. Verjullo-Silva, M. Linardi and E. Spinace, *Ionics*, 2010, **16**, 85–89.
- 106 M. Y. Zhu, G. Q. Sun and Q. Xin, *Electrochim. Acta*, 2009, **54**, 1511–1518.
- 107 F. J. R. Varela and O. Savadogo, *Asia-Pac. J. Chem. Eng.*, 2009, **4**, 17–24.
- 108 P. E. Tsiakaras, *J. Power Sources*, 2007, **171**, 107–112.
- 109 J. Ribeiro, D. M. dos Anjos, K. B. Kokoh, C. Coutanceau, J. M. Leger, P. Olivi, A. R. de Andrade and G. Tremiliosi-Filho, *Electrochim. Acta*, 2007, **52**, 6997–7006.
- 110 H. Q. Li, G. Q. Sun, L. Cao, L. H. Jiang and Q. Xin, *Electrochim. Acta*, 2007, **52**, 6622–6629.
- 111 E. Antolini, F. Colmati and E. R. Gonzalez, *Electrochem. Commun.*, 2007, **9**, 398–404.

- 112 S. Rousseau, C. Coutanceau, C. Lamy and J. M. Leger, *J. Power Sources*, 2006, **158**, 18–24.
- 113 S. Q. Song, W. J. Zhou, Z. X. Liang, R. Cai, G. Q. Sun, Q. Xin, V. Stergiopoulos and P. Tsiakaras, *Appl. Catal., B*, 2005, **55**, 65–72.
- 114 Z. L. Liu, X. Y. Ling, X. D. Su, J. Y. Lee and L. M. Gan, *J. Power Sources*, 2005, **149**, 1–7.
- 115 W. J. Zhou, S. Q. Song, W. Z. Li, Z. H. Zhou, G. Q. Sun, Q. Xin, S. Douvartzides and P. Tsiakaras, *J. Power Sources*, 2005, **140**, 50–58.
- 116 F. Vigier, C. Coutanceau, A. Perrard, E. M. Belgsir and C. Lamy, *J. Appl. Electrochem.*, 2004, **34**, 439–446.
- 117 N. Fujiwara, Z. Siroma, S. I. Yamazaki, T. Ioroi, H. Senoh and K. Yasuda, *J. Power Sources*, 2008, **185**, 621–626.
- 118 H. Y. Hou, G. Q. Sun, R. H. He, Z. M. Wu and B. Y. Sun, *J. Power Sources*, 2008, **182**, 95–99.
- 119 D. Gaurava, A. Verma, D. K. Sharma and S. Basu, *Fuel Cells*, 2010, **10**, 591–596.
- 120 S. Y. Shen, T. S. Zhao, J. B. Xu and Y. S. Li, *J. Power Sources*, 2010, **195**, 1001–1006.
- 121 J. B. Xu, T. S. Zhao, S. Y. Shen and Y. S. Li, *Int. J. Hydrogen Energy*, 2010, **35**, 6490–6500.
- 122 L. An, T. S. Zhao, R. Chen and Q. X. Wu, *J. Power Sources*, 2011, **196**, 6219–6222.
- 123 L. An, T. S. Zhao and J. B. Xu, *Int. J. Hydrogen Energy*, 2011, **36**, 13089–13095.
- 124 H. Y. Hou, S. L. Wang, Q. A. Jiang, W. Jin, L. H. Jiang and G. Q. Sun, *J. Power Sources*, 2011, **196**, 3244–3248.
- 125 H. Y. Hou, S. L. Wang, W. Jin, Q. Jiang, L. L. Sun, L. H. Jiang and G. Sun, *Int. J. Hydrogen Energy*, 2011, **36**, 5104–5109.
- 126 Y. S. Li and T. S. Zhao, *Int. J. Hydrogen Energy*, 2011, **36**, 7707–7713.
- 127 J. Datta, A. Dutta and M. Biswas, *Electrochem. Commun.*, 2012, **20**, 56–59.